Received: 29 April 2020 | Revised: 29 July 2020 | Accepted: 31 July 2020

DOI: 10.1111/bre.12504

ORIGINAL ARTICLE

Basin Research | IAS EAGE | WILEY

The Middle Jurassic to lowermost Cretaceous in the SW Barents Sea: Interplay between tectonics, coarse-grained sediment supply and organic matter preservation

Dora Marín[1] | **Solveig Helleren**[1] | **Alejandro Escalona**[1] | **Snorre Olaussen**[2] | **Andrés Cedeño**[1] | **Henrik Nøhr-Hansen**[3] | **Sverre Ohm**[1]

[1]Department of Energy Resources, University of Stavanger, Stavanger, Norway

[2]Department of Arctic Geology, University Centre in Svalbard (UNIS), Longyearbyen, Norway

[3]Geological Survey of Denmark and Greenland (Geus), Kobenhavn, Denmark

Correspondence
Dora Marín, University of Stavanger, 4036, Stavanger, Norway.
Email: doraluzmr@gmail.com

Funding information
JuLoCrA consortium

Abstract

Syn-rift successions contain both prolific organic-rich and coarse-grained rocks, but these rocks are usually studied independently. Thus, the interplay among organic matter deposition, tectonics and sediment supply is not commonly assessed. In this study, we use well logs, Total Organic Carbon (TOC) content, biostratigraphy and seismic data from the SW Barents Sea to unravel the variability of organic-rich successions and its interaction with potential reservoir rocks in areas affected by active normal faulting versus tectonically stable areas. Four Transgressive-Regressive (T-R) sequences were defined for the Middle to Upper Jurassic Fuglen Formation and for the organic-rich Upper Jurassic to lowermost Cretaceous Hekkingen Formation. Three TOC trends, controlled by palaeobathymetric variations, and organic matter dilution, were identified within the two main organic-rich sequences (sequences 2 and 3): (a) wells with the highest TOC values (>10 wt %) at the base of the succession; (b) wells with the highest TOC values at the top of the succession and (c) wells with high TOC values at the base and top of the succession. Our interpretation indicates that fault activity controlled the TOC trends in two different ways: Firstly, by creating a sharp topographic contrast-triggering hyperpycnal flows, and shallowing the footwalls, where higher oxygen content and less developed stratified waters lowered organic matter preservation. Secondly, by significantly increasing the input of clastic material, which inherently led to dilution of organic matter and resulted in lower TOC values (<6 wt %). We interpret that sand deposition was controlled by the size and geomorphology of the sediment source areas. The western part of the study area (i.e. the Loppa High) was characterized by uplifted footwall islands and localized sands along their flanks, whereas the southern part (i.e. the Finnmark Platform) constituted a larger sediment source area for the Volgian age. This work has implications for a better understanding of the distribution of reservoir and source rocks in active rift basins.

1 | INTRODUCTION

Prolific source rocks are commonly deposited alternating with syn-rift sandstone in active rift basins (Huc, le Fournier, Vandenbroucke, & Bessereau, 1990; Ravnås & Steel, 1998). The coexistence of organic-rich and coarse-grained rocks is well known in areas such as the North Sea, and other localities of the Norwegian Continental Shelf (NCS), where the Upper Jurassic succession constitutes both a reservoir target and a main source rock (e.g. fields such as the Brae in the UK sector of the North Sea; and Borg, Troll, Johan Sverdrup and Draugen fields on the NCS; Chiarella, Longhitano, Mosdell, & Telesca, 2020; Goesten & Nelson, 1992; Scott & Ottesen, 2018; Turner & Hooper, 2018). Previous studies have described the impact of sediment input on the dilution and preservation of organic matter, the role of basin physiography and stratified water column in the distribution of organic matter and how high subsidence together with starving sediment conditions contribute to the formation of organic-rich rocks in rift basins (van Buchem, Herbin, de Boer, McCave, & Huc, 1995; Herbin et al., 1995; Huc et al., 1990; Katz, 1995; Macquaker & Gawthorpe, 1993; Ravnås & Steel, 1997; Tyson, 1996). However, syn-rift coarse-grained and organic-rich rocks are usually studied separately. Regional studies on organic-rich rocks deposited in marine rift basins have largely focused on geochemical characterization or on the cyclicity of these rocks, mainly neglecting the role of tectonics.

Upper Jurassic syn-rift wedge-shaped geometries have been imaged in seismic lines adjacent main fault complexes in the SW Barents Sea (Blaich, Tsikalas, & Faleide, 2017; Kairanov, Marín, Escalona, & Cardozo, 2019; Serck, Faleide, Braathen, Kjølhamar, & Escalona, 2017) and localized sandstone units have been penetrated by exploration wells (e.g. wells 7120/2-2 and 7120/12-1; Braut, 2018; NPD, 2020; Sandvik, 2014). In addition, the Upper Jurassic to lowermost Cretaceous succession of the SW Barents Sea hosts a prolific source rock in the region, known as the Hekkingen Formation (Lerch, Karlsen, Matapour, Seland, & Backer-Owe, 2016; Lerch et al., 2018; Mørk et al., 1999). Compositional variations in the Hekkingen Formation are well known in the area (e.g. Ohm, Karlsen, & Austin, 2008; Smelror, Mørk, Mørk, Weiss, & Løseth, 2001). Løseth, Wensaas, Gading, Duffaut, and Springer (2011a) described four main TOC patterns in the Upper Jurassic organic-rich formations of the NCS: upward increasing, blocky, bell-shaped and upward decreasing patterns. The upward decreasing TOC pattern was associated with the Hekkingen Formation (Løseth et al., 2011a). However, this work focused on the geophysical response and did not present further interpretations of these TOC trends. Helleren, Marín, Ohm, Augustsson, & Escalona, (2020) analysed the geochemistry of two of the maximum flooding surfaces (MFSs) defined in this current study. This study concluded that variations in uranium, as a response of

Highlights

- TOC trends in organic-rich successions were controlled by palaeobathymetry and dilution.
- Similar TOC trends are observed in tectonically active and stable areas, but TOC values are different.
- The input of coarse-grained material was controlled by the sediment source size.

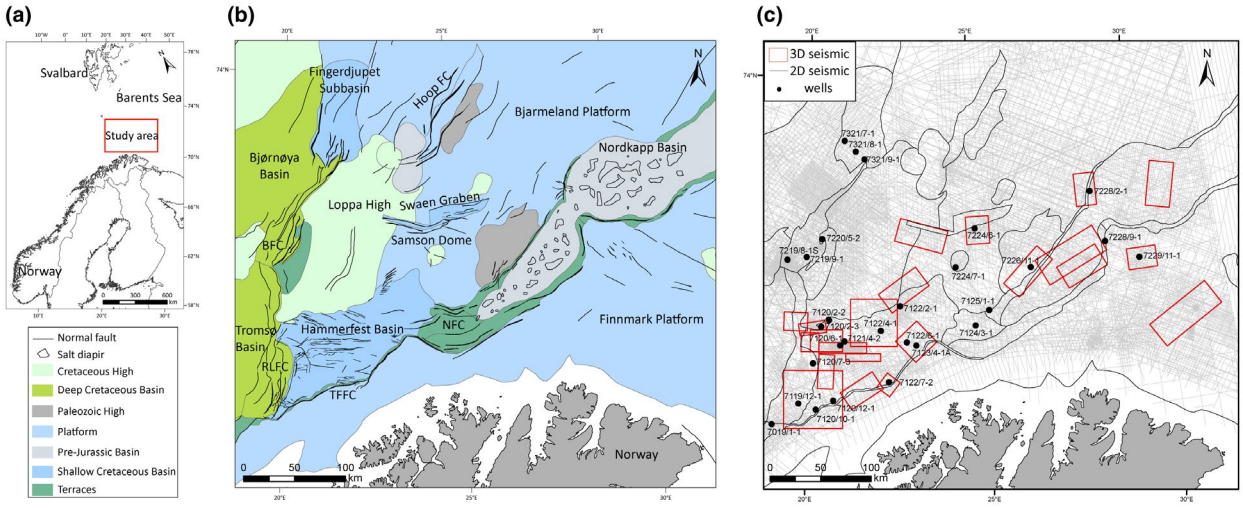

FIGURE 1 (a) Location of the study area. (b) Structural elements of the south-western Barents Sea (Adapted from NPD, 2020; using data from Marín et al., 2018b; Usken, 2018; Josefsen, 2019). TFFC: Troms Finnmark Platform; RLFC: Ringvassøy-Loppa Fault Complex; BFC: Bjørnøyrenna Fault Complex; NFC: Nysleppen Fault Complex. C) Dataset used in this study

fluctuations in sea level and redox conditions, controlled the intensity in the GR spikes at the location of MFSs. However, a proper analysis of the variation in the TOC trends of these rocks within a sequence stratigraphic framework, together with a thorough understanding of regional geology and tectonics, has not yet been published.

A detailed analysis of the Middle Jurassic to the lowermost Cretaceous succession, in the SW Barents Sea, represents a unique opportunity to better understand the variability of organic-rich successions and their interaction with potential reservoirs in active rift basins (Figure 1). Particularly, the findings in this study have implications for predicting preferential accumulation areas of the more prolific source rocks in sediment-balanced to sediment-underfilled marine rift basins (Ravnås & Steel, 1998). The main objectives of this study are as follows: 1) to define a sequence stratigraphic framework and analyse the variation in TOC trends in the SW Barents Sea; 2) to unravel how active tectonics control the variations in these TOC trends, and the input of coarse-grained sediments and 3) to improve the palaeogeographic understanding of the SW Barents Sea during the Middle Jurassic to the earliest Cretaceous.

1.1 | Sequence stratigraphy and distribution of organic-rich successions

Previous studies have applied sequence stratigraphy to correlate organic-rich successions (e.g. Abouelresh & Slatt, 2012; Bohacs et al., 2005; van Buchem et al., 1995; Creaney & Passey, 1993; Hemmesch, Harris, Mnich, & Selby, 2014; Herbin et al., 1995; Koevoets, Hammer, Olaussen, Senger, & Smelror, 2018; Surlyk, 1991; Tyson, 1996). These rocks exhibit many challenges that need to be considered, such as:

1. Cyclicity in organic-rich rocks normally correlates with relative sea-level variations in anoxic sea floor conditions. Commonly high TOC values are linked to maximum flooding surfaces, but they are not always necessarily correlative (Bohacs et al., 2005; Hemmesch et al., 2014; Herbin et al., 1995). Organic-rich intervals have also been reported in regressive periods, particularly over distal marine areas (Bohacs et al., 2005; Hemmesch et al., 2014). Local and seasonal events such as algae bloom, upwelling and variation in precipitation, salinity, wind and nutrient input from rivers can cause water stratification and increase organic matter productivity in a basin (van Buchem et al., 1995; Koevoets et al., 2018; Macquaker & Gawthorpe, 1993; Nagy, Reolid, & Rodríguez-Tovar, 2009; Tyson & Pearson, 1991).
2. The methodology to establish sequence boundaries includes identification of strata termination and stacking patterns using seismic data, well logs and outcrops (Catuneanu et al., 2009; Mitchum, Vail, & Sangree, 1977). Well logs, particularly the gamma-ray (GR) log, have been extensively used to define stacking patterns in areas where outcrops are not available (e.g. Davies & Elliott, 1996; Martins-Neto & Catuneanu, 2010; Miller et al., 2013). Organic-rich rocks usually exhibit high GR log values due to high uranium content. However, uranium is a mobile element, therefore, organic-rich rocks do not always correlate with high GR values (Abouelresh & Slatt, 2012; Bowker & Grace, 2010; Rider, 1996; Helleren, et al., 2020).
3. Organic-rich rocks are fine grained and mostly deposited in anoxic sea floor conditions, usually without clear indicators of palaeobathymetry. Therefore, it is a challenge to define retrogradational and progradational patterns based on outcrop or core data (Surlyk, 1991).
4. Biological productivity in shallow marine and shelf areas is higher than in deep marine settings (Tissot & Welte, 1984; Tyson & Pearson, 1991). However, in shallow marine conditions, coarser-grained sediment and higher oxygen content inhibit or decrease the preservation of organic matter (van Buchem et al., 1995; Herbin et al., 1995; Khan, Ansari, & Lyla, 2012; Tyson, 1996). In deep marine conditions, lower biological productivity and a higher water column can affect the generation and preservation of organic matter (Bohacs et al., 2005; Demaison & Moore, 1980).
5. Isolated basins with prevailing reducing conditions commonly develop in rift basins, where the subsidence rate exceeds the input of sediment (Hunt, 1995). These isolated basins tend to be ideal settings for the accumulation and preservation of organic matter (Hunt, 1995). However, high sedimentation rates can contribute to low preservation of organic matter due to dilution (Katz, 1995) and uplifted footwalls might create hyperpycnal flows bringing oxygenated water to the sea floor (Lash, 2016; Macquaker & Gawthorpe, 1993).

2 | GEOLOGICAL SETTING

2.1 | Tectonic setting

The western margin and southern part of the SW Barents Sea has experienced different extensional events from the late Palaeozoic to the Tertiary (Berglund, Augustson, Færseth, Gjelberg, & Ramberg-Moe, 1986; Faleide, Vågnes, & Gudlaugsson, 1993; Gernigon et al., 2014; Sund, Skarpnes, Jensen, & Larsen, 1986). One of the extensional events occurred during the Middle Jurassic to Early Cretaceous, affecting basins such as the Hammerfest, Tromsø, Bjørnøya and Nordkapp (Figures 1b and 2; Berglund et al., 1986; Blaich et al., 2017;

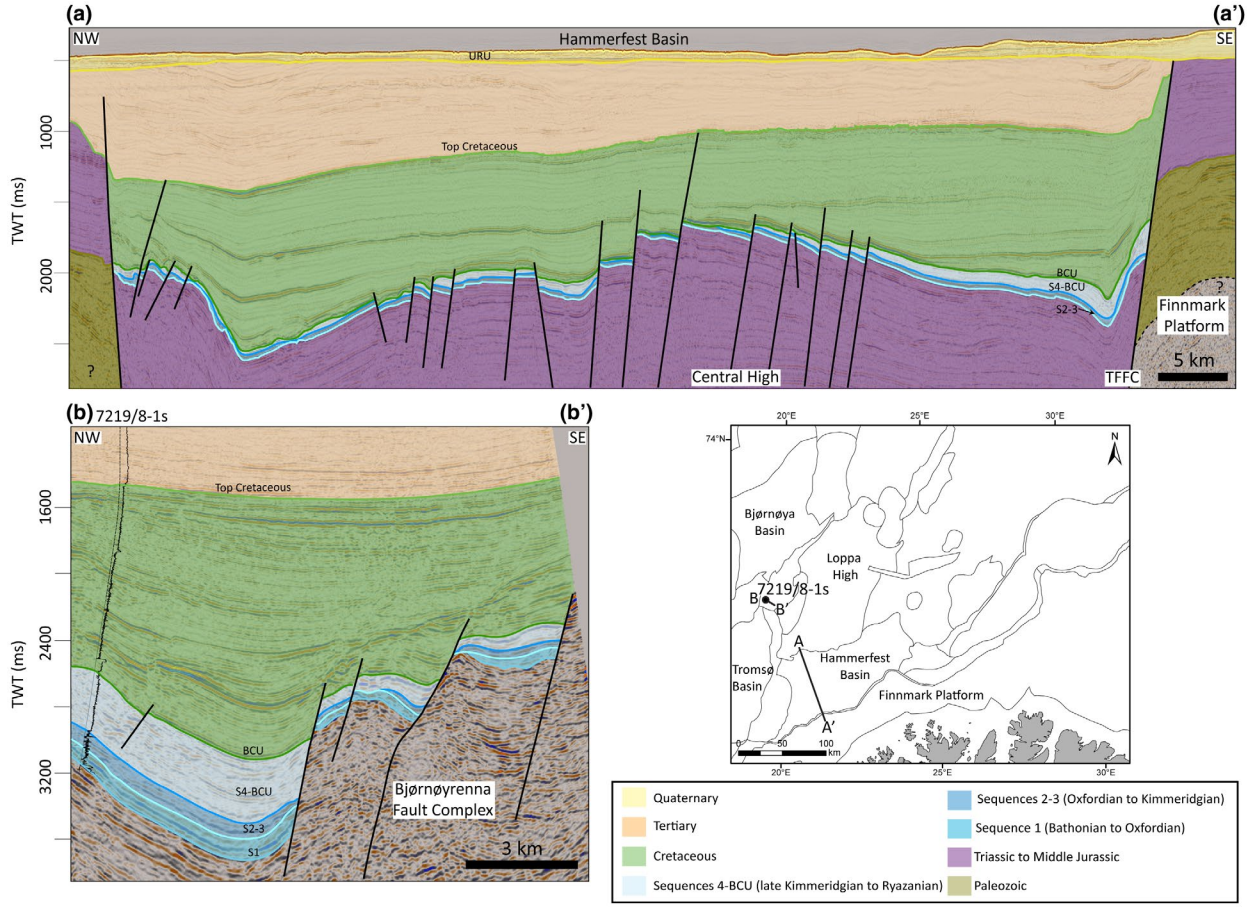

FIGURE 2 Regional cross sections showing the Middle Jurassic to lowermost Cretaceous succession. A-A' section along the Finnmark Platform, the Hammerfest Basin and the southern part of the Loppa High. B-B' section along the Bjørnøyrenna Fault Complex. URU: Upper Regional Unconformity; BCU: Base Cretaceous Unconformity

Clark et al., 2014; Faleide et al., 1993; Kairanov et al., 2019; Marín et al., 2018b; Rojo, Cardozo, Escalona, & Koyi, 2019; Serck et al., 2017; Sund et al., 1986). The initiation of this extensional phase has been interpreted as Bathonian to Callovian, marked by a regional unconformity between the Stø and Fuglen formations boundary (Figure 3b; Faleide et al., 1993; Klausen, Müller, Poyatos-Moré, Olaussen, & Stueland, 2019; Mulrooney, Leutscher, & Braathen, 2017). However, the timing of the initiation of this event is difficult to constrain in the different basins of the SW Barents Sea due to the lack of age control, and because the Middle to the lowermost Cretaceous succession is thin and some of the formations can be below seismic resolution (Figures 2 and 3). An Aptian-Albian extensional phase affected the western flank of the Loppa High, the Fingerdjupet Subbasin and the Hoop Fault Complex (Figure 1b; Faleide et al., 2019; Marín, Escalona, Grundvåg, Nøhr-Hansen, & Kairanov, 2018a; Serck et al., 2017). During these extensional phases, fault complexes such as the Ringvassøy-Loppa, Troms Finnmark and Bjørnøyrenna were active (Blaich et al., 2017; Faleide et al., 1993; Kairanov et al., 2019; Marín et al., 2018a). The Loppa High is interpreted to have been uplifted during the Late Jurassic to Early Cretaceous (Berglund et al., 1986; Glørstad-Clark, 2010; Sund et al., 1986). More recently, the initiation of this uplift event has been interpreted as early Barremian (Indrevær, Gabrielsen, & Faleide, 2017) or latest Jurassic (Marín et al., 2018a). Uplift in the central part of the Hammerfest Basin started during the Middle Jurassic according to Berglund et al. (1986).

2.2 | Stratigraphy

The upper Middle Jurassic to lowermost Cretaceous succession has been divided into two formations in the SW Barents Sea, the Bathonian to Oxfordian Fuglen Formation and Oxfordian to Ryazanian Hekkingen Formation (Dalland, Worsley, & Ofstad, 1988; Mørk et al., 1999; Figure 3b). These formations are time equivalent to the Agardhfjellet Formation in Spitsbergen (Grundvåg et al., 2017; Koevoets et al., 2018; Mørk et al., 1999). The Fuglen Formation is composed of mudstone, and thin very fine-grained sandstone and limestone beds (Mørk et al., 1999). This formation has been interpreted as deposited in an inner shelf environment, and beneath the storm wave base in well 7122/7-2 in the

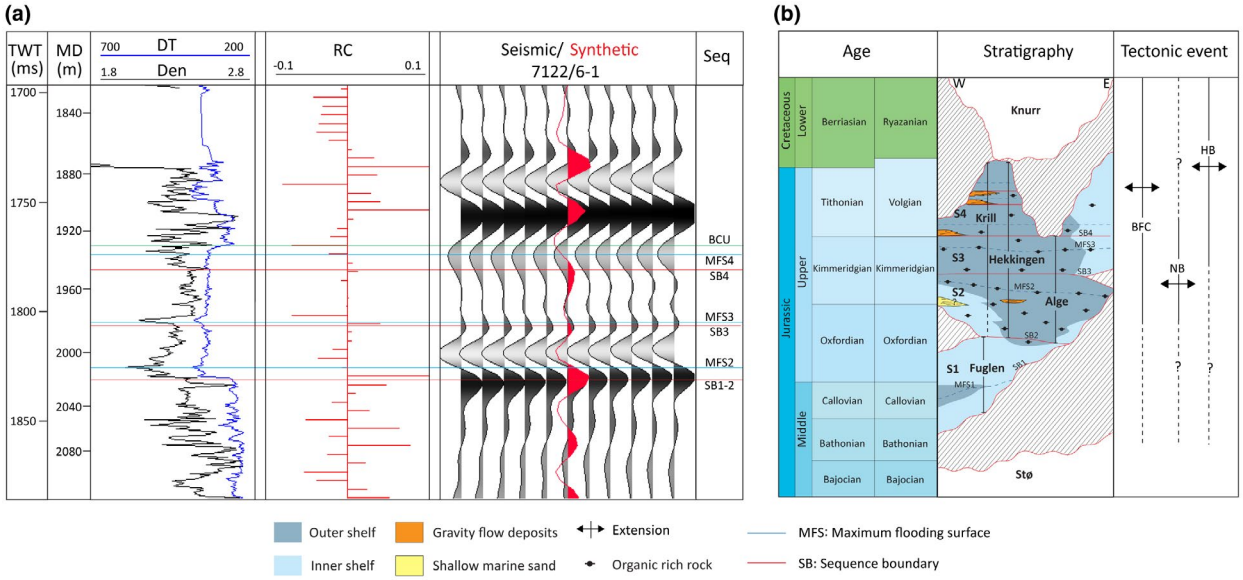

FIGURE 3 (a) Synthetic seismogram showing that some of the tops are below the limit of separability and they cannot be mapped as individual reflectors. (b) Middle Jurassic to lowermost Cretaceous formations and the sequences (S1–S4) interpreted in this study. BFC: Bjørnøyrenna Fault Complex; NB: Nordkapp Basin; HB: Hammerfest Basin. Adapted from Grundvåg et al. (2017) with the data from this study and from Århus (1991); Bugge et al. (2002); Wierzbowski and Smelror (2020)

southern part of the Hammerfest Basin (Mørk et al., 1999; Mulrooney et al., 2018). Based on well logs, the thickness of the Fuglen Formation varies from 48 m in the southern part of the Hammerfest Basin to less than 10 m in the central high of the Hammerfest Basin (Dalland et al., 1988; Mørk et al., 1999). The base of the Fuglen Formation is marked by a hiatus near the Bajocian to Bathonian boundary, but can also span from late Rhaetian–early Callovian in areas such as the Goliat Field in the southern part of the Hammerfest Basin (Mørk et al., 1999; Mulrooney et al., 2018). The Hekkingen Formation is divided into two members: Alge and Krill (Figure 3b). The Alge Member is composed of organic-rich shale of late Oxfordian to Kimmeridgian age and usually exhibits high GR log values (Dalland et al., 1988; Georgiev et al., 2017; Mørk et al., 1999; Smelror et al., 2001). The Alge Member has been interpreted as deposited in a marine shelf mostly under anoxic sea floor conditions (Mørk et al., 1999). Distal gravity flow deposits have been described in well 7219/8-1s, located to the west of the Loppa High (Figures 1,2; Helleren, et al., 2020). The Krill Member is composed of shale (TOC between 2% to 6%; Henriksen et al., 2011), siltstone and minor sandstone units of Kimmeridgian to Ryazanian age (Braut, 2018; Georgiev et al., 2017; Mørk et al., 1999). Gravity flow deposits have been described in the Krill Member in wells 7120/2-2 and 7120/12-1 in the northern and southern part of the Hammerfest Basin (Figure 1; Braut, 2018; Sandvik, 2014). The depositional environment of the Krill Member is interpreted as below or near storm wave base on a marine shelf, probably as a distal prograding shelf. The thickness of the Hekkingen Formation varies from 856 m in well 7219/8-1s, located in the Bjørnøyrenna Fault Complex, to less than 100 m in some areas of the Hammerfest Basin (Figures 1 and 2b; Dalland et al., 1988; NPD, 2020). The base and the top of the Hekkingen Formation are characterized by hiatuses spanning from Callovian to middle Oxfordian, and Kimmeridgian to Ryazanian or Barremian age, respectively (Figure 3b; Bugge et al., 2002; Marín et al., 2018b; Wierzbowski & Smelror, 2020). Palynostratigraphic and other biostratigraphic information (e.g. ammonites) from the Fuglen and Hekkingen formations has been previously published by Wierzbowski and Århus (1990); Smelror and Below (1993); Smelror and Dypvik (2005); Bugge et al. (2002); Wierzbowski and Smelror (2020).

3 | DATA AND METHODS

3.1 | Dataset

Twenty-eight wells were used in this study (Figure 1c). All wells contain a full set of logs, and three wells have spectral GR logs available (7220/5-2, 7224/6-1 and 7120/2-3s). TOC measurements were obtained from various geochemical reports available on the NPD factpages (https://factpages.npd.no/factpages/; wells 7120/10-1, 7120/7-3, 7120/6-1, 7121/4-2, 7122/4-1, 7122/6-1, 7124/3-1, 7125/1-1, 7224/7-1, 7226/11-1, 7229/11-1, 7228/9-1, 7228/2-1, 7219/9-1, 7321/7-1, 7321/8-1 and 7321/9-1) and from in-house studies belonging to the JuLoCrA consortium (https://wp.ux.uis.no/julocra/) acquired by Applied Petroleum Technologies (APTEC; wells 7119/12-1, 7220/5-2, 7224/6-1, 7120/12-1, 7120/2-3s and 7219/8-1s). TOC measurements correspond

to both cuttings and sidewall cores. In-house TOC measurements were carried out using a Leco SC-632 instrument and the amount of organic carbon in the sample was measured by an IR-detector. The TOC data available in the NPD factpages were obtained by eliminating the inorganic carbon with HCl and the amount of organic carbon was measured using a LECO Carbon analyser (NPD, 2020). The sampling interval varies from 2 m to 20 m.

We used 22 three-dimensional seismic datasets and more than 1,000 two-dimensional seismic lines, covering an area of 150000 km^2. The dataset was provided by the Norwegian National Data Repository Diskos database (Figure 1c). The seismic is shown in positive polarity, where an increase in acoustic impedance is displayed as a positive peak in blue colour. The seismic vertical resolution was calculated by λ/4, where λ = velocity/frequency. Seismic resolution is usually around 20 m at the level of interest, using an interval velocity of 2930 m/s and a frequency of 35 Hz.

3.2 | Methodology

In this study, we implemented T-R sequences (Embry, 2009) in an attempt to build correlations with previous studies in the Arctic region that have applied similar sequence stratigraphic schemes for the Jurassic successions (e.g. Koevoets et al., 2018; Smelror et al., 2001). To define the sequence stratigraphic framework, we utilized a combination of well logs including spectral GR, Th/K and Th/U ratios, GR, density logs, resistivity and sonic logs overlay (sonic log in reverse scale), along with TOC data. A visual calibration was performed between the TOC measurements obtained from both cuttings and sidewall cores and well logs. High TOC measurements positively correlate with greater separation between resistivity and sonic logs, with low-density values and low Th/K ratio. The correlation between TOC measurements and GR log varies from good (e.g. wells 7119/12-1, 7224/6-1) to poor (e.g. wells 7120/2-3s and 7220/5-2; see Appendix S1). For the sequence definition, we interpreted progradational and retrogradational patterns in the well logs. Four main sequences were defined (sequences 1 to 4). The sequence boundaries are called SB1 to SB4 and the maximum flooding surfaces are called MFS1 to MFS4. Sequence boundaries (SBs) correspond to the maximum regressive surface (Embry, 2009), and may coincide with a subaerial unconformity. In this work, sequence boundaries are interpreted when there is a change from progradational to retrogradational pattern, a minimum separation between the resistivity and sonic log (reverse scale), high Th/K ratio and low TOC values. Maximum flooding surfaces are interpreted when there is a change from retrogradational to progradational pattern, high GR values and low-density readings coinciding with high TOC values. A large separation between the resistivity and sonic logs indicates high TOC values, commonly suggesting maximum flooding conditions (Creaney & Passey, 1993; Passey, Creaney, Kulla, Moretti, & Stroud, 1990). Spectral GR (containing measurements of potassium, thorium and uranium) has been used to interpret sedimentation rates. Potassium and thorium are indicative of higher sedimentation rates, whereas uranium tends to be deposited in periods of condensed sedimentation rates (Abouelresh & Slatt, 2012; Paxton et al., 2007). In addition, the Th/K ratio tends to be higher in shallow marine than in deep marine conditions (Myers & Wignall, 1987). Thus, MFSs are usually associated with low sedimentation rates and low Th/K ratio (deeper conditions; Emery & Myers, 2009; Smelror et al., 2001).

In order to constrain the age of the sequences in the Hammerfest Basin and in the eastern part of the study area, we used palynological analysis available in the Diskos database (NPD, 2020). Particularly well 7120/12-1 was crucial for this purpose because it contains the well type section for the Hekkingen Formation (NPD, 2020). The reflectors in this area are relatively continuous and mappable, and the Oxfordian to Kimmeridgian succession normally displays high TOC values, which strengthen our interpretations in this area. In the western flank of the Loppa High, the age control was scarce, the seismic interpretation was more challenging because structural complexities and the Oxfordian to Kimmeridgian succession has lower TOC content. Therefore, we included the biostratigraphic analysis of well 7220/5-2 located in this western flank. The biostratigraphic interpretation of well 7220/5-2 is based on a StrataBugs v2.0 DEXFile with palynomorph occurrences from 200 samples produced by Robertson Ltd and available in the Diskos database. The samples include both the Jurassic and the Cretaceous. The interpretation of the Cretaceous samples was previously published in Marín et al. (2018a). Based on the publicly available biostratigraphic information (i.e. Diskos database) and the information produced in this study, the sequences have a duration of approximately 4 Myr, between Bathonian and Ryazanian. Two intra-Volgian sequences were locally identified in the south-western part of the Hammerfest Basin (sequences 5 and 6), but they were not interpreted in the seismic lines because their lack of lateral continuity.

Seismic interpretation of sequences 1 to 4 was challenging because in some parts of the study area these sequences are below or at the limit of separability and cannot be mapped as an individual reflector (Figure 3a). Therefore, the reflectors mapped in this study are called: (a) near SB2, which mainly comprises the SB2; however, sequence 1 is commonly below or at the limit of seismic resolution, hence, this reflector could include SB1, MFS1 and MFS2 (Figure 3a); (b) near MFS3 (late Kimmeridgian), which includes MFS3 and in some cases SB3 (Figure 3a) and (c) Base Cretaceous Unconformity (BCU), corresponds to the top of the Hekkingen Formation. The thickness map for

sequence 1 was built using exclusively well tops because a large part of this sequence is below seismic resolution. A time thickness map was created using the seismic interpretation between the tops near SB2 and near MFS3, representing approximately the time thickness of both sequences 2 and 3. A second thickness map was made using the seismic interpretation between the tops near MFS3 and BCU, representing approximately the time thickness of sequence 4. Finally, three palaeogeographic maps were created based on the interpretation presented in this study, integrated with previously published core descriptions (Braut, 2018; Bugge et al., 2002; Helleren, et al., 2020; Sandvik, 2014). To constrain the palaeogeographic interpretations, in particular, the uplift of the Finnmark Platform in the southern part of the study area, we include a list of reworked Jurassic fossils identified in two samples from the Cretaceous Knurr Formation from well 7019/1-1 (2232.55 and 2224.25 m).

4 | REVISED BIOSTRATIGRAPHY OF TWO WELLS ON THE WESTERN MARGIN

4.1 | Well 7220/5-2

Based on well log data, the top of the Hekkingen Formation (BCU) is interpreted at 1391 m (NPD, 2020). Below this boundary, the succession is interpreted as Kimmeridgian in age indicated by the last occurrence (LO) of *Gonyaulacysta jurassica* and of *Rhynchodiniopsis cladophora* at 1393 m (Appendix S2). The succession from 1393 to 1411 m has been interpreted as Kimmeridgian. The succession from 1411 to 1567 m has questionably been interpreted as Oxfordian–Callovian. The LO of *Endoscrinium galeritum* at 1411 m indicates early Kimmeridgian age (cymodoce standard (ammonite) Zone according to Costa and Davey (1992)). However, the early Kimmeridgian records are inconsistent, and this species is especially characteristic of the late Callovian to Oxfordian (Riding & Fensome, 2002). The presence of in situ *Nannoceratopsis pellucida* at 1441 m may indicate the lowermost Kimmeridgian baylei standard (ammonite) Zone according to Costa and Davey (1992). However, this species may be common in the Callovian of the Barents Sea region (Smelror & Below, 1993). The LO of *Trichodinium scarburghense* in situ at 1447 m and the LO of *Rigaudella aemula* at 1477 m indicate middle Oxfordian according to Costa and Davey (1992), and the LO of *Lithodinia jurassica* at 1489 m suggests an early Oxfordian age according to Smelror and Below (1993); whereas the LO of *Paragonyaulacysta calloviensis* at 1459 m indicates a Callovian age according to Smelror and Below (1993). The succession from 1567 to 1700 m has been interpreted as Bajocian. The LO of consistent *Nannoceratopsis senex* at 1567 m may indicate a middle Bajocian age according to Smelror and Below (1993); whereas the LO of *Phallocysta elongata* and *Moesiodinium raileanui* at 1585 m suggests an early Bajocian age according to Riding (1994) and Costa and Davey (1992), respectively, and the LO of *Mancodinium semitabulatum* at 1633 m also suggests an early Bajocian age according to Costa and Davey (1992).

4.2 | Well 7019/1-1 (Jurassic reworked material in Lower Cretaceous wedges)

Well 7019/1-1 is located in the western flank of the Finnmark Platform (Figure 1). The Jurassic reworked material identified within the synrift Lower Cretaceous Knurr Formation helps to interpret the sediment that was deposited in the Finnmark Platform during the Middle Jurassic to lowermost Cretaceous. Two samples from the interval 2232.55 m to 2224.25 m were analysed in the Knurr Formation. The dinocyst assemblage (*Pseudoceratium nudum, Pseudoceratium tovae, Circulodinium* aff. *C. attadalicum, Hystrichosphaerina schindewolfii*) in the first sample (2232.55 m) suggests late Barremian to earliest Aptian (dinocyst Subzone I (3) and questionable lower part of Zone II of Nøhr-Hansen, 1993). The youngest sample from the Knurr Formation (2224.25 m) is dominated by corroded Early to Middle Jurassic dinocysts: *Nannoceratopsis gracilis* (Pliensbachian–Bathonian), *Nannoceratopsis pellucida* (Bajocian–Kimmeridgian) and *Nannoceratopsis ridingii* (Pliensbachian–Aalenian). Volgian and Lower Cretaceous dinocysts were not observed in this sample. One possible interpretation is that Jurassic dinocysts in the youngest sample are redeposited.

5 | DESCRIPTION OF SEQUENCES

5.1 | Sequence 1 (Bathonian–Oxfordian)

The sequence boundary surface 1, SB1, is marked by a hiatus in most of the Barents Sea (e.g. well 7120/2-3s located in the Hammerfest Basin; Figure 4), and as in Svalbard represents a subaerial unconformity followed by a transgressive bed (Klausen et al., 2019; Rismyhr, Bjærke, Olaussen, Mulrooney, & Senger, 2019 and references therein).

5.1.1 | Well log character

Sequence boundary 1 (SB1) is characterized by low uranium, potassium, thorium and GR values, a minimum separation between the resistivity and sonic logs, a high Th/K ratio and low Th/U ratio (Figure 4). From SB1, the potassium and

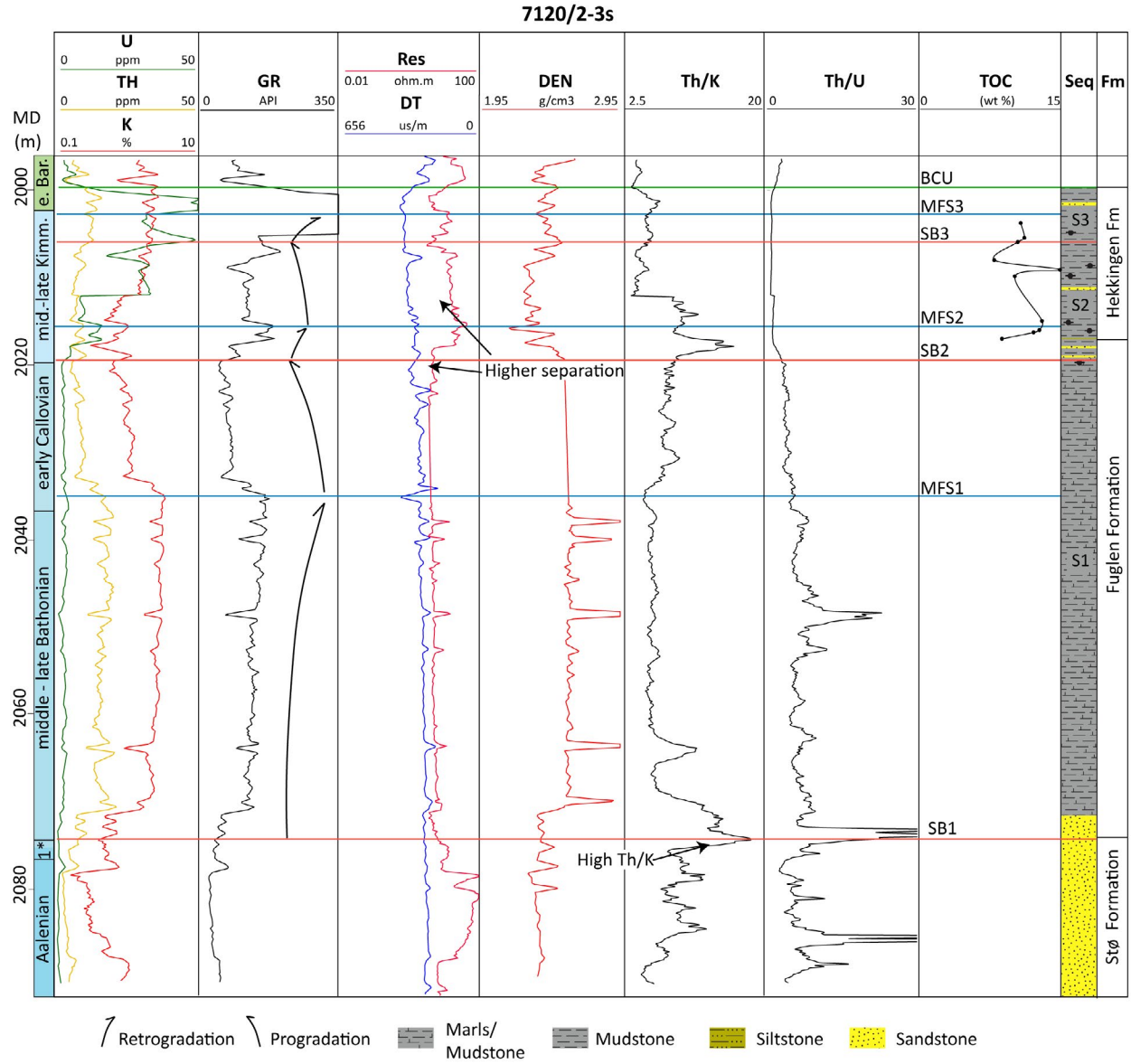

FIGURE 4 Sequence stratigraphic framework defined in well 7120/2-3s. SB: sequence boundary; MFS: maximum flooding surfaces. High Th/K ratio at the location of SB1 indicates a shallow palaeowater depth. High separation between the resistivity and sonic logs suggests higher content of organic matter. Age information was obtained from the Diskos database. Lithology adapted from Braut (2018) and Helleren et al. (2020). 1* Aalenian/Bathonian

total GR values increase gradually upward to the location of MFS1. The Th/K ratio shows an upward decreasing trend. MFS1 is characterized by high potassium and high GR values, a higher separation between the resistivity and sonic logs and a low Th/K ratio. The succession between MFS1 and SB2 is characterized by an upward decreasing trend in the potassium and thorium logs and in the GR log. The Th/K ratio exhibits a well-defined increasing upwards trend, whereas the Th/U ratio shows a decreasing upwards trend. Uranium values remain low and constant in sequence 1 (Figure 4). The resistivity and sonic log separation is usually low in sequence 1, except at MFS1 and at the top of the sequence before SB2 (Figure 4). Sequence 1 is composed of marls, mudstones and thin layers of carbonates (Figure 7; NPD, 2020).

Interpretation

High Th/K ratio at the location of SB1 could indicate a shallow palaeowater depth for the area around well 7120/2-3s, as has been suggested by Myers and Wignall (1987) for the Kimmeridge Clay. The separation between the resistivity and sonic logs at the top of the sequence suggests that the organic matter content is increasing towards the top of sequence 1 (Figure 4).

5.1.2 | Thickness

Sequence 1 is absent in the southern part of the study area and in the Loppa High (Figure 5a). In most of the study

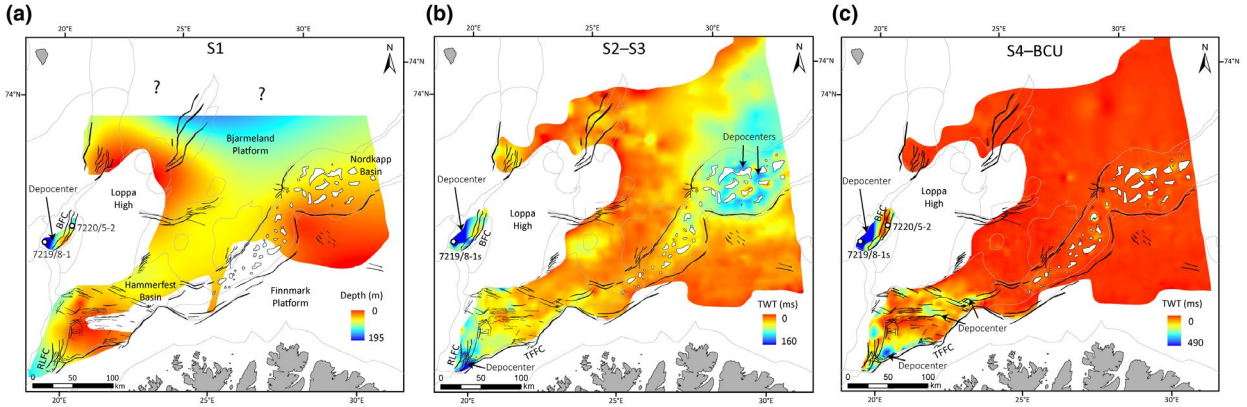

FIGURE 5 (a) Thickness map for sequence 1 (Bathonian–Oxfordian) based on well tops (base and top of sequence 1). (b) Time thickness map for sequences 2 and 3 (Oxfordian–Kimmeridgian) based on seismic interpretation. (c) Time thickness map for sequences 4 to BCU (late Kimmeridgian–Ryazanian) based on seismic interpretation

area (the Hammerfest Basin, the Bjarmeland Platform and the Nordkapp Basin), the thickness of sequence 1 is relatively constant with a mode value of 35 m, with some minor variations between the south-western and central part of the Hammerfest Basin. In contrast, sequence 1 is thicker along the Bjørnøyrenna Fault Complex and with highly variable thicknesses, for instance, in wells 7219/8-1s and 7220/5-2, it varies from 193 and 68 m respectively (Figure 5a).

5.1.3 | Seismic character

Sequence 1 is usually below or at the limit of seismic resolution, which is approximately 20 m. However, in areas such as the south-western Hammerfest Basin and along the Bjørnøyrenna Fault Complex, it is possible to map the top and base of this sequence. Along the Bjørnøyrenna Fault Complex, both tabular packages with constant thickness and

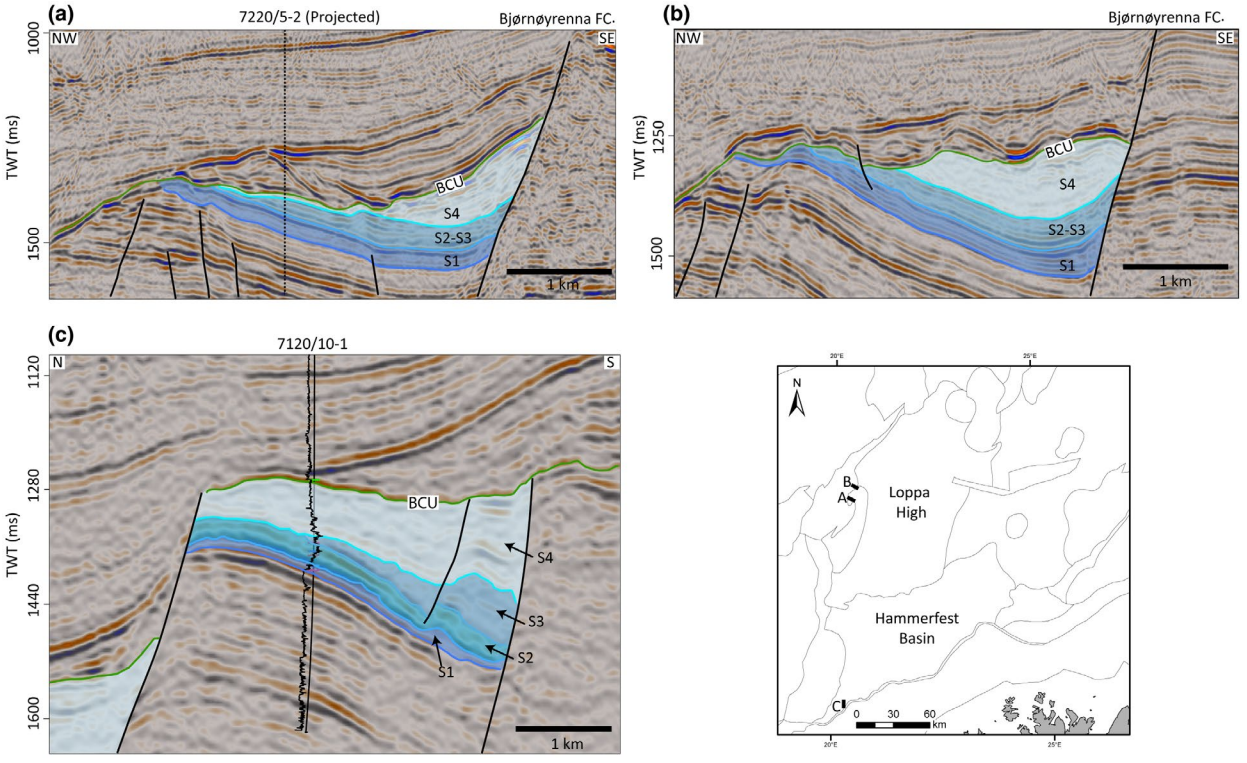

FIGURE 6 Seismic character of the sequences along the Bjørnøyrenna Fault Complex. (a) Sequence 1 shows a tabular geometry, whereas sequences 2 to BCU exhibit a wedge-shaped geometry. (b) Thickness variation and wedge-shaped geometries are observed in all the sequences, including sequence 1. (c) Seismic line along the Troms Finnmark Fault Complex. Sequences 1 and 2 show tabular geometries. Sequences 3 and 4 show wedge-shaped units

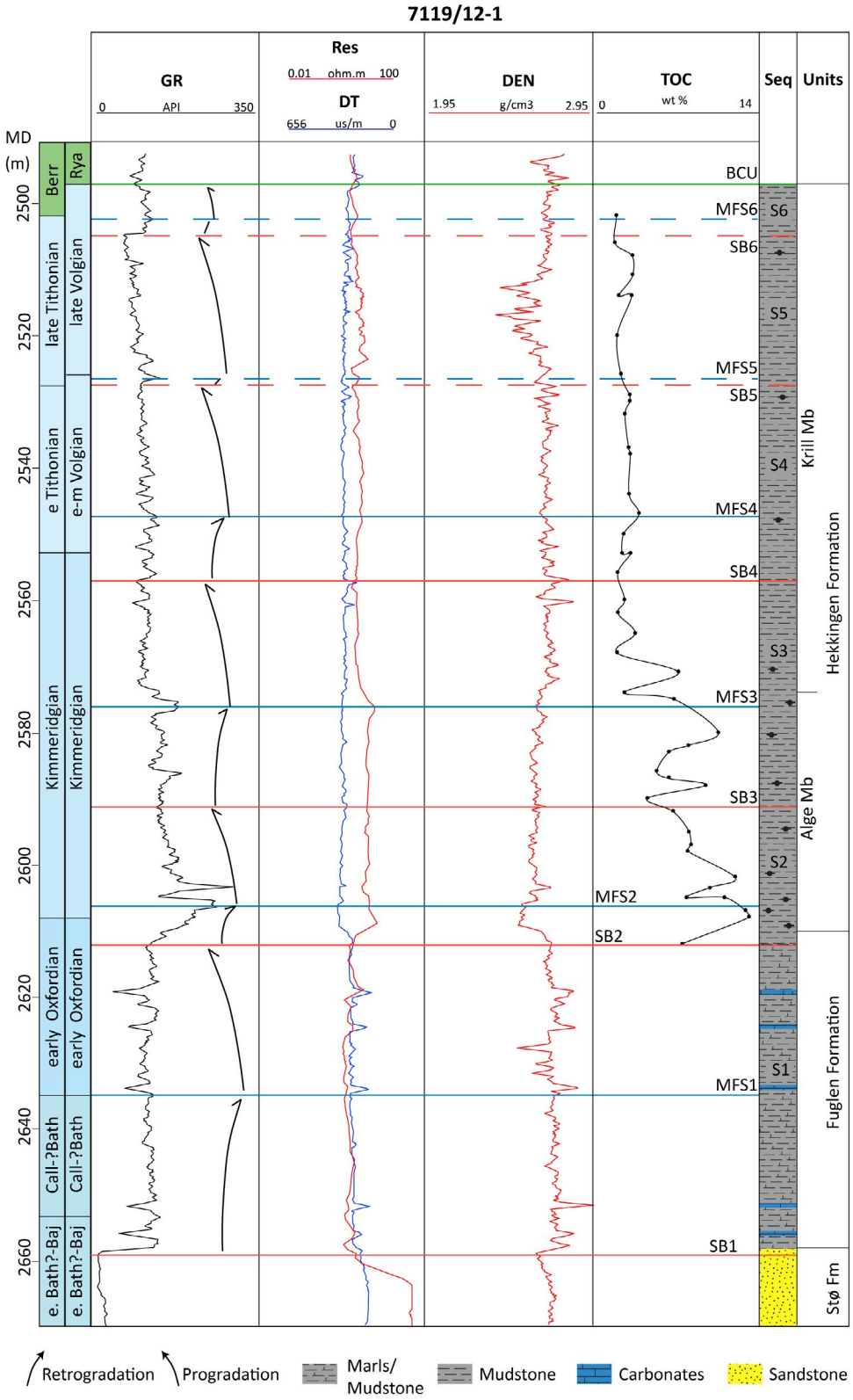

FIGURE 7 Sequence stratigraphic framework defined in well 7119/12-1. MFS, maximum flooding surfaces; SB, sequence boundary. Age information was obtained from the Diskos database. Lithology from cutting descriptions (NPD, 2020). TOC sample location is indicated with black circles

small wedge-shaped geometries are locally interpreted in sequence 1 (Figures 2b, 6a,b, Appendix S3). In the south-western Hammerfest Basin, sequence 1 has a tabular geometry and wedge-shaped geometries were not observed (Figure 6c).

Interpretation of thickness variations and seismic character

Thickness variation and the presence of local wedges along the Bjørnøyrenna Fault Complex indicate that this fault

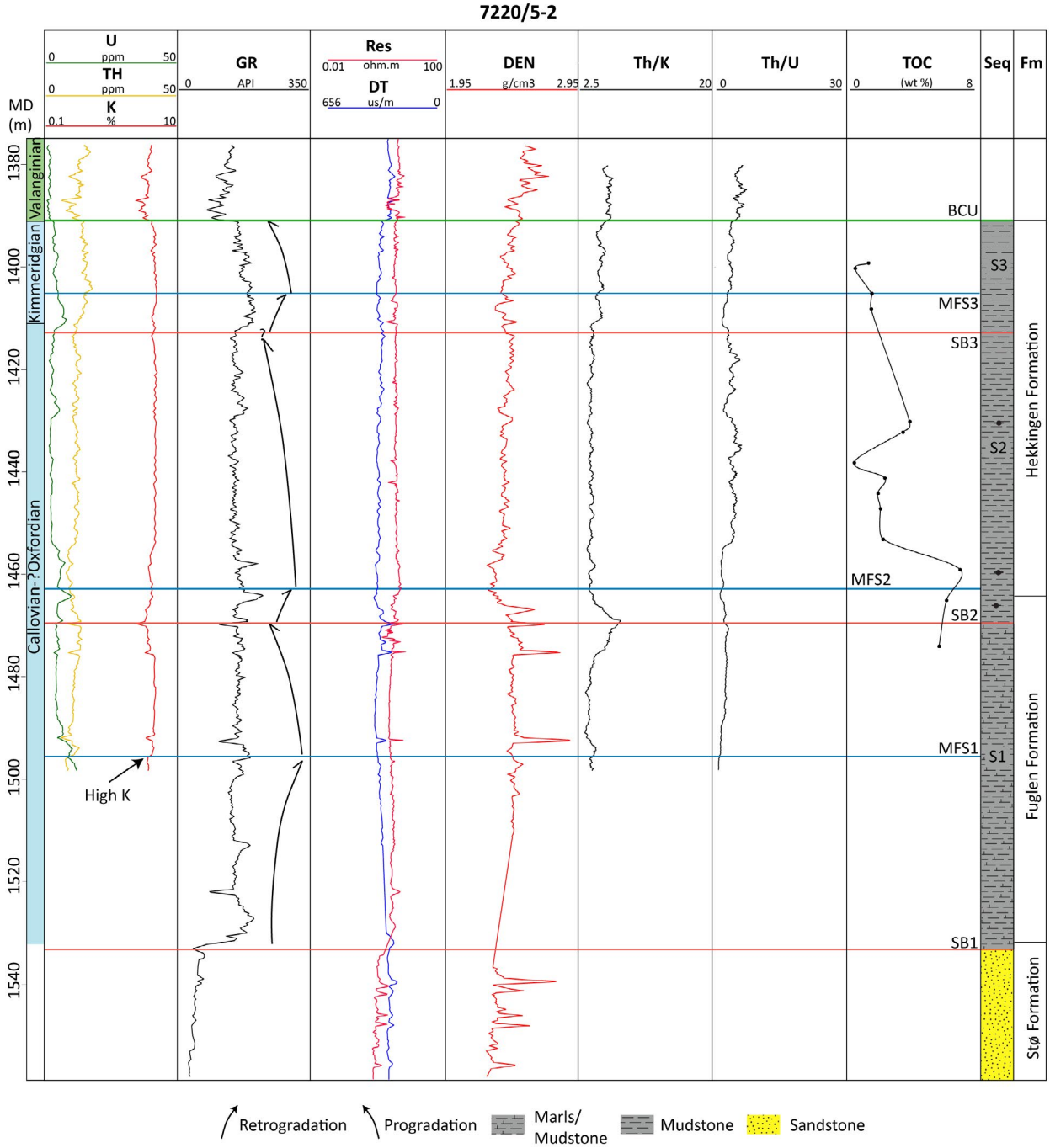

FIGURE 8 Sequence stratigraphic framework defined in well 7220/5-2. MFS, maximum flooding surfaces; SB, sequence boundary. Note that the TOC values are lower than 8 wt %. High TOC values are observed at MFS2. High potassium content is interpreted due to fast sedimentation rates. Lithology interpreted from well logs

complex could have been active during deposition of sequence 1 (Figures 5a and 6b). The absence of this sequence in the southern part of the Hammerfest Basin could also be related to active tectonism (Figure 5a). However, the absence of wedge-shaped geometries (Figure 6c) indicates that faulting during deposition of sequence 1 was minor in the Hammerfest Basin.

5.2 | Sequences 2 and 3 (Oxfordian–Kimmeridgian)

The sequence boundary surface 2, SB2, marked a sudden change in lithology from silty mudstone to black organic-rich mudstone often with a hiatus dated in "mid" Oxfordian in southern part of Barents Sea (Smelror et al., 2001). The

surface is probably diachronous based on palynology in well 7119/12-1 (middle-early Oxfordian to earliest Kimmeridgian; Figure 7).

5.2.1 | Well log character

The base of sequence 2 is defined by SB2, which coincides often with a hiatus dated based on palynology (Figures 3 and 4). SB2 has a similar response to SB1, which is characterized by low uranium, potassium, thorium and GR values, a minimum separation between the resistivity and sonic logs, density, Th/K ratio is high and the Th/U ratio is low (Figures 4, 7, 8). A thin succession from SB2 to MFS2 shows upwards increasing values in potassium, uranium, GR and decreasing values in density and in the Th/K ratio. MFS2 is characterized by prominent high values in the GR, a large separation between resistivity and sonic logs, low Th/K ratio and low-density values. MFS2 has the highest TOC values (more than 10 wt %) in the studied succession for wells located in the southern part of the study area, particularly at the borders of the Hammerfest Basin (black dots in Figure 9). MFS2 also has the highest TOC values in the studied succession in most of the wells located to the west of the Loppa High. However, TOC values are usually lower than 6 wt % in wells located closer to the western faulted flank of the Loppa High (wells 7220/5-2, 7321/9-1 and 7321/8-1; Figure 9).

The base of sequence 3 is marked by SB3, which coincides with a hiatus in well 7220/5-2 (Figure 8). SB3 is interpreted based on the low values in the GR, a slight increase in the Th/K ratio and low TOC values (Figures 4, 7, 8). From MFS2 to MFS3, potassium and uranium logs show an overall increasing upwards trend and separation between resistivity and sonic logs remains high, but decreases in SB3 (Figures 4, 7). MFS3 displays a high separation between the resistivity and sonic logs, low-density values and low Th/K ratio, and a second prominent spike in the uranium and GR logs. MFS3 has the highest TOC values (more than 10 wt %) for wells 7124/3-1 and 7226/11-1, located in the south-eastern part of the study area (red dots in Figure 9). MFS3 also has the highest TOC values in the studied succession in well 7219/9-1 located in an uplifted footwall to the west of the Loppa High, but TOC values are lower (4.8 wt %; Figure 9c).

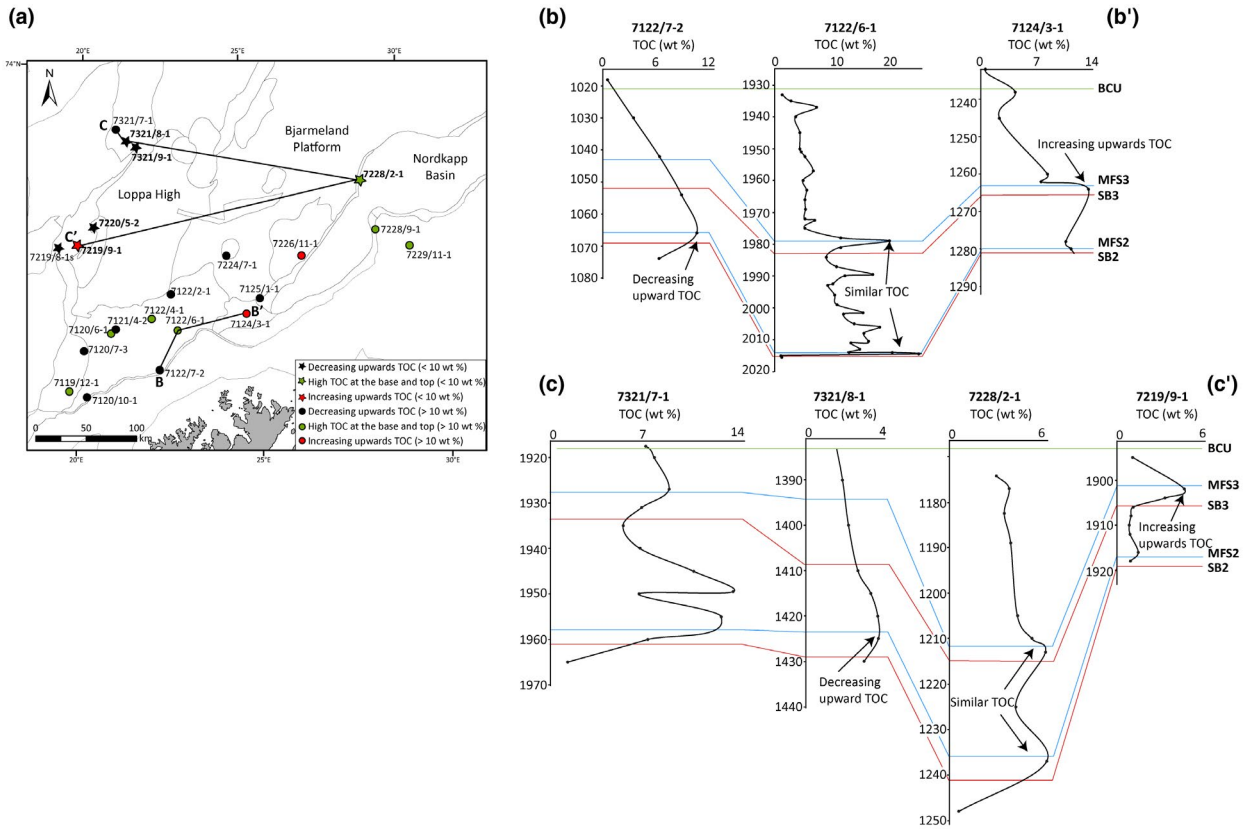

FIGURE 9 (A) Distribution of the three different TOC trends identified in this study. (B) TOC trends identified in the tectonically stable areas or areas affected by minor faulting. (C) TOC trends identified in the area adjacent active faults. Note that similar trends are observed in the tectonically stable and tectonically active areas, but the TOC content is lower in the tectonic active area due to organic matter dilution. TOC data from NPD (2020)

Other wells located in the southern and eastern part of the study area have TOC values above 10 wt % in both MFS2 and MFS3 (green dots in Figure 9a). The thorium log presents relatively constant values in sequences 2 and 3, slightly increasing towards the top of sequence 3. In these two sequences, the Th/U ratio exhibits low and relatively constant values in wells located to the west of the Loppa High and consistently high potassium (Figure 6). Wells located in the Bjarmeland Platform have low and constant potassium values (Figure 10). Wells 7220/5-2 and 7224/6-1 show minor TOC increments at 1430 m and 945 m, respectively (Figures 8 and 10). Sequences 2 and 3 are mainly composed of organic-rich mudstones, and thin layers of sandstone are also present (Figures 4 and 7).

Interpretation of well character

The high separation between the resistivity and sonic logs, in addition to high TOC values, suggest that sequences 2 and 3 contain the highest amount of organic matter in the studied succession. The variation in the TOC content among MFS2 and MFS3, differences in TOC trends (Figure 9), and lower TOC values in the wells located to the west of the Loppa High reflect lateral and vertical compositional variations in these two Oxfordian to Kimmeridgian sequences (Figures

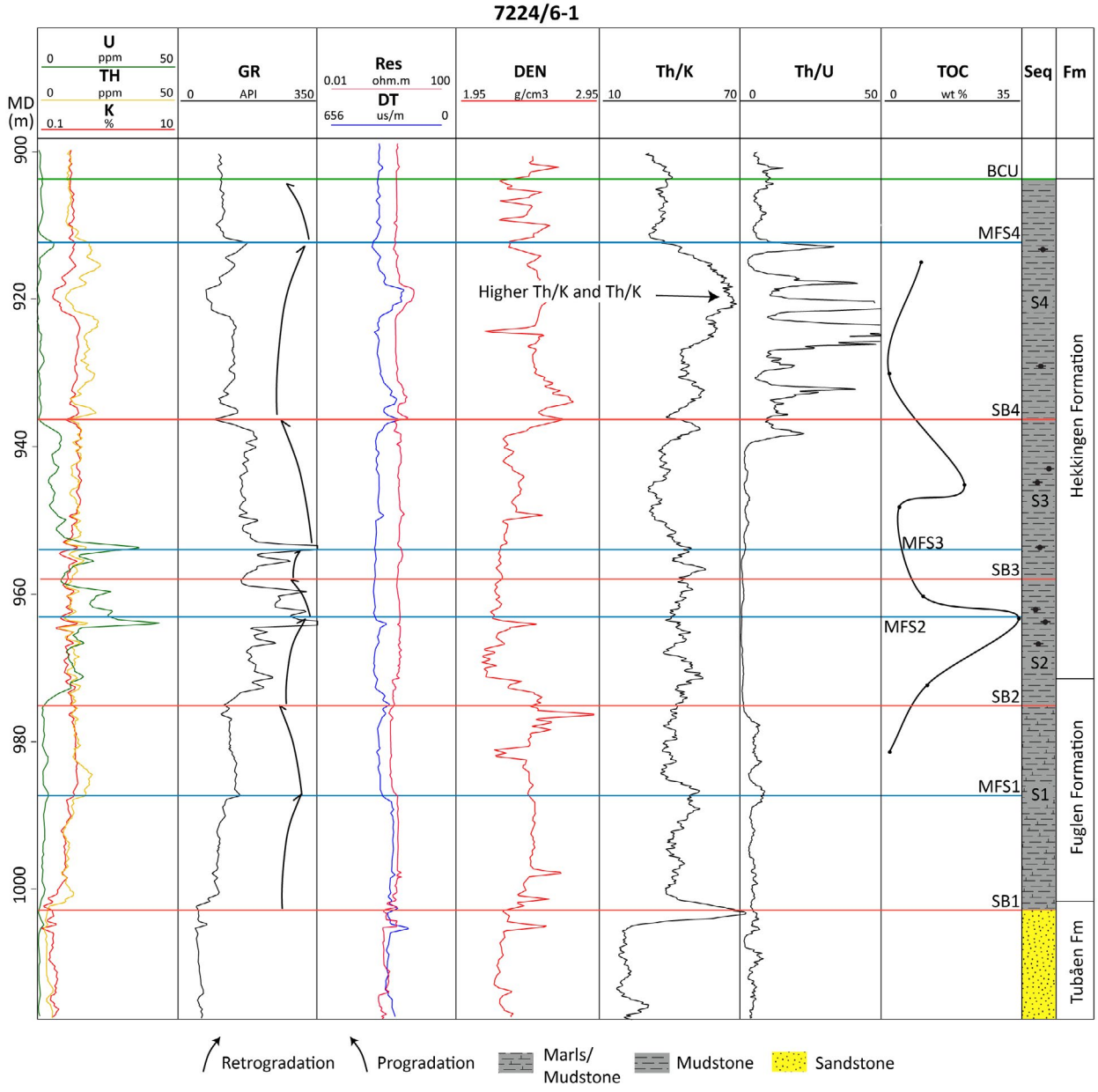

FIGURE 10 Sequence stratigraphic framework defined in well 7224/6-1. SB: sequence boundary; MFS: maximum flooding surfaces. High Th/K and Th/U ratios could reflect the input of a new source of sediment (i.e. Loppa High) and higher sedimentation rates. Lithology interpreted from well logs

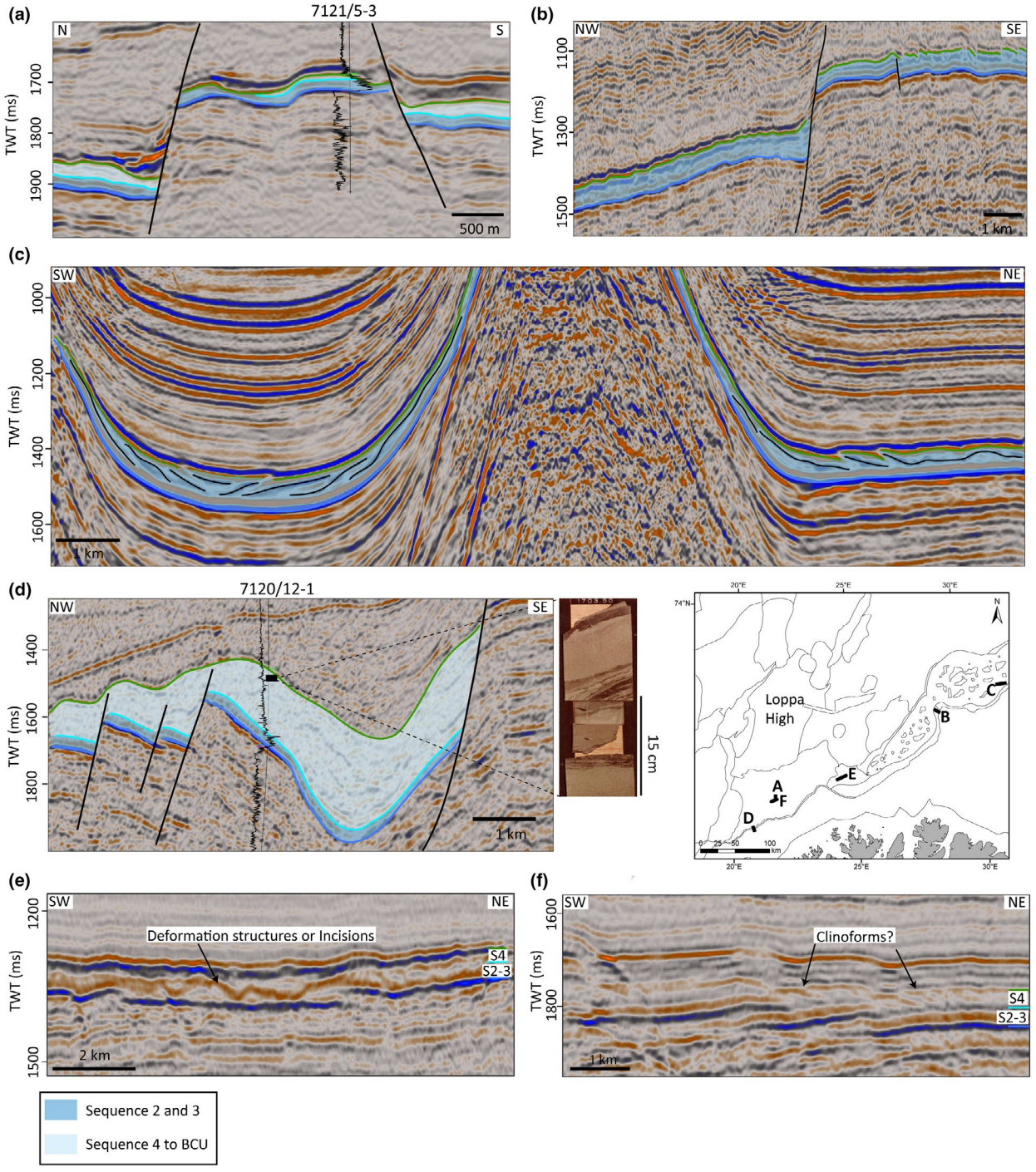

FIGURE 11 Seismic character of sequences 2 to BCU. (a) Constant thickness of sequences 2 and 3, and thickness variation in sequences 4 to BCU are observed in the central high of the Hammerfest Basin. (b) Thickness variation and wedge-shaped geometries are observed in sequences 2 and 3 in the boundary faults of the Nordkapp Basin. (c) Wedge-shaped geometries observed along the salt diapir flanks in the Nordkapp Basin. (d) Thickness variation and wedge-shaped geometries in sequences 4 to BCU are observed in the south-western Hammerfest Basin. Well 7120/12-1 penetrated gravity flow deposits in the upper part of these sequences (Braut, 2018; NPD, 2020). (e) Wavy internal character interpreted as deformation structures. (f) Incline reflectors interpreted as clinoforms, where the progradation of sediments was triggered by recently uplifted footwalls

4, 7–10). The minor increments observed in the TOC data of wells 7220/5-2 and 7224/6-1 show that enrichment of TOC may also occur in any part of the sequence, not only at the MFSs (Figures 8 and 10), as previously documented by Bohacs et al. (2005). The relatively low Th/K ratio at SB3 contrasts with comparatively higher values observed at SB1 and SB2 (Figure 4). This could reflect deeper sedimentary conditions during the Kimmeridgian, even

during SB3, relative to the late Bathonian and Oxfordian (SB1 and SB2).

5.2.2 | Thickness

Sequences 2 and 3 are absent or below seismic resolution on highs and part of platforms in areas such as the Loppa High, part of the Finnmark Platform and to the northeast of the Loppa High (Figure 5b). The time thickness map for sequences 2 and 3 shows a relatively constant thickness in the Bjarmeland Platform and in most of the Hammerfest Basin 36 m (25 ms). The thickness of these sequences increases around the Ringvassøy-Loppa Fault Complex and in the south-western portion of the Troms-Finnmark Fault Complex, where values around 40 m (27 ms) are interpreted (Figure 5b). Thickness variations are observed in the Nordkapp Basin related to normal faults and within salt mini-basins (Rojo et al., 2019). Additionally, the thickest interval of these sequences is observed along the hanging wall of the Bjørnøyrenna Fault Complex, where a succession of 185 m (105 ms) was drilled in well 7219/8-1s (Figures 2b, 5b). Wells such as 7220/5-2 and 7219/9-1 are located in uplifted footwalls. The top of the sequences in this area is a regional unconformity (BCU); where the Volgian succession can be absent in these uplifted blocks (Figures 6 and 8). The thickness of sequences 2 and 3 in wells 7220/5-2 and 7219/9-1 is 79 m (52 ms) and 25 m (16 ms) respectively (Figures 6 and 8).

5.2.3 | Seismic character

Sequences 2 and 3 have been interpreted in the entire Hammerfest Basin, in the central high and in the basin boundaries with relatively constant thickness (Figure 11a,d). In the south-western part of the Hammerfest Basin sequences 2 and 3 are above seismic resolution (Figure 6c). Sequence 2 shows a tabular geometry and high amplitude. Sequence 3 exhibits thickness variations, wedge-shaped geometries and has lower amplitudes than sequence 2 (Figure 6c, Appendix S3). Thickness variations and wedge-shaped geometries are observed along the Bjørnøyrenna Fault Complex and in the boundary faults of the Nordkapp Basin (Figures 6a,b and 11b). Additionally, wedge-shaped geometries are observed on the flanks of salt diapirs in the Nordkapp Basin (Figure 11c, Appendix S4). Internally, sequences 2 and 3 have high amplitude, and wavy reflectors are common (Figure 11e,f).

Interpretation of thickness variations and seismic character

Thickness variation and seismic wedges observed along the Bjørnøyrenna Fault Complex and in the boundary faults of the Nordkapp Basin indicate fault activity during the deposition of sequences 2 and 3 (Blaich et al., 2017; Serck et al., 2017; Figures 6 and 11b). Peridiapiric wedges on the flanks of salt diapirs in the Nordkapp Basin indicate halokinetic movements, as interpreted by Rojo et al. (2019; Figure 11c). The constant thickness, and tabular geometry observed in sequence 2 in the south-western Hammerfest Basin, suggests tectonically stable conditions (or only minor fault activity; Figures 6c and 11a). Wedge-shaped geometries indicate that the southern boundary faults of the Hammerfest basin were active during the deposition of sequence 3. Lower amplitudes in sequence 3 compared to sequence 2 suggest that the organic matter is less condensed in sequence 3 in the southern Hammerfest Basin. Wavy reflectors are interpreted as faulted beds, where the offset of the faults is below seismic resolution. Similar structures were described by Løseth, Wensaas, and Gading (2011b). Alternatively, these wavy reflectors can represent incisions (Figure 11e).

5.3 | Sequence 4 to BCU (late Kimmeridgian–Ryazanian)

5.3.1 | Well log character

Sequences 4 to BCU are characterized by slightly irregular, but relatively constant values in the GR log (Figure 7). There is a separation between the resistivity and sonic logs, but it is not as evident as in sequences 2 and 3. TOC values are lower than in the two previous sequences (Figure 7). In sequences 4 to BCU, there is a considerable increase in thorium, and the uranium content decreases, which is reflected by higher Th/K and Th/U ratios (Figure 10). A similar trend is observed in the Hammerfest Basin wells with available spectral GR logs (e.g. 7123/4-1A). Sequences 4 to BCU are absent in wells 7120/2-3s and 7220/5-2 (Figures 4 and 8). In well 7119/12-1 two additional sequences are interpreted (sequences 5 and 6), but they are not present in the other wells analysed in this study. Sequence boundaries SB4, SB5 and SB6 have low values in the GR log, low separation between the resistivity and sonic logs and relatively high-density values (Figure 7). Maximum flooding surfaces MFS4, MFS5 and MFS6 show high values in the GR log (but not as high as MFS2 and MFS3), medium separation between the resistivity and sonic logs and relatively low values in the density log. Sequence 4 to BCU is composed of mudstones, siltstone and minor units of sandstones (NPD, 2020).

Interpretation of well log character

The higher content of thorium in these sequences may be indicative of a new sediment source and higher sedimentation rates (Figure 10; Abouelresh & Slatt, 2012; Paxton et al., 2007). This can be explained by an increase in tectonic

activity in the Hammerfest Basin, the Loppa High and the Swaen Graben (Figure 1). A lower separation between the resistivity and sonic logs together with lower TOC and uranium values indicate comparatively less amount of organic matter than in previous sequences. However, TOC values are above 2% in several places.

5.3.2 | Thickness

Similar to previous sequences, sequences 4 to BCU are absent in the Loppa High, part of the Finnmark Platform and to the northeast of the Loppa High (Figure 5c). These sequences exhibit the highest contrast in thickness variation in areas such as the Hammerfest Basin, where the thickness varies from absent in well 7120/2-3s to 60 m (41 ms) in well 7119/12-1 (Figure 7). The main depocenters are clearly aligned with the main faults, and thicker successions are observed in graben areas and in the hanging wall of the Troms-Finnmark Fault Complex. Along the Bjørnøyrenna Fault Complex, a thickness of 671 m (362 ms) has been interpreted in well 7219/8-1s (Figure 2b), but sequences 4 to BCU are partially absent in the uplifted footwalls (e.g. well 7220/5-2). In the Bjarmeland Platform, the Finnmark Platform and the Nordkapp Basin, the thickness of these sequences is relatively constant (20 ms).

5.3.3 | Seismic character

Sequences 4 to BCU display the largest thickness variations in areas such as the Hammerfest Basin and the Bjørnøyrenna Fault Complex (Figure 11a,d). Wedge-shaped geometries are observed along the Bjørnøyrenna Fault Complex and in the hanging wall of the faults of the Hammerfest Basin. They are particularly dominant along the Troms-Finnmark Fault Complex to the south of the basin where sandstone and siltstone packages of around 3 m have been penetrated (well 7120/12-1; Figures 6 and 11d; Braut, 2018; NPD, 2020). Thin lamina of siltstone has also been penetrated in a Volgian-Ryazanian wedge in the southern flank of the Loppa High (well 7120/2-2; Sandvik, 2014). Internally, these sequences tend to have lower amplitude compared to sequences 2 and 3, and incline reflectors have been observed in the Hammerfest Basin (Figure 11f).

Interpretation of thickness variations and seismic character

The existence of wedge-shaped geometries and thickness variation suggests that this was a period of fault activity in the Hammerfest Basin and the Bjørnøyrenna Fault Complex (Serck et al., 2017). The lower amplitude of these sequences compared to sequences 2 and 3 is consistent with a general lower content of organic matter, a more heterolithic succession and coarser-grained siliciclastic content. Incline reflectors are interpreted as clinoforms, reflecting sediment progradation from recently uplifted footwalls in the central part of the Hammerfest Basin.

6 | DISCUSSION

6.1 | Controls on vertical and lateral variation in TOC trends

For the high organic-rich sequences 2 and 3 (Oxfordian to Kimmeridgian), three different TOC trends were identified: (a) wells with decreasing upwards TOC values, where the highest TOC occurs at the base of the organic-rich succession at MFS2, as documented in well 7122/7-2, near Troms Finnmark Fault Complex (TFFC; Figures 1 and 9b); (b) increasing upwards TOC values, where the highest TOC is dominant at the top of the succession at MFS3, as in well 7124/3-1, located in the Nysleppen Fault Complex; (c) a combination of 1 and 2 with high TOC at the base in MFS2 and at the top in MFS3, as shown in well 7122/6-1 (Figure 9b). These three different TOC trends were identified for both tectonically stable areas or affected by only minor faulting (i.e. the Hammerfest Basin and the Bjarmeland and Finnmark platforms); and in tectonically active area (i.e. western flank of the Loppa High and the Nordkapp Basin). However, in wells located adjacent main active faults, the TOC is <6 wt % at the MFSs (e.g. wells 7321/8-1, 7228/2-1 and 7219/9-1), in contrast to the tectonically stable areas, where TOC is usually >10 wt % at the MFSs (Figure 9c).

6.1.1 | Tectonically stable areas or affected by minor faulting

Based on the observations in this study, the three TOC trends observed in the tectonically stable areas or areas affected by minor faulting (i.e. pre rift, cf. Prosser, 1993) can be explained by an interplay between palaeobathymetry and dilution of organic matter, which concurs with previous studies such as van Buchem et al. (1995) and Herbin et al. (1995). The TOC trends can partially be explained following the model proposed by Helleren, et al., (2020), where the variations in uranium content could explain the changes in the magnitude of GR spikes at MFS2 and MFS3, as a result of fluctuations in the redox conditions and in the sea level. However, this model does not discriminate between active tectonic areas and tectonically stable areas, and it includes neither the role of differential subsidence (e.g. growth fault basins) nor the variation in sediment input.

1. TOC trend 1: wells with decreasing upwards TOC values, where MFS2 coincides with the highest TOC (> 10 wt %), tend to be located within the main depocenters of sequences 2 and 3 (e.g. hanging walls close to the master faults of the Hammerfest Basin), where sequence 3 is thicker than sequence 2 (Figures 6c and 9). The wedge-shaped geometries observed in the south-western Hammerfest Basin during sequence 3, the decreasing upwards TOC profiles, the relatively low TOC content at MFS3 and a thicker sequence 3 in the wells with this TOC trend suggest that the normal faults became active during sequence 3. This fault activity triggered higher subsidence, increased clastic input and led to higher dilution of organic matter in sequence 3 relative to sequence 2 (Figure 6c).
2. TOC trend 2: wells with increasing upwards TOC values, where MFS3 displays the highest TOC values (> 10 wt %), are located where sequence 1 is absent. These areas are interpreted to have been subaerially exposed during sequence 1, and began to be flooded during sequence 2 (Figures 5a and 9; Berglund et al., 1986; Bugge et al., 2002; Klausen et al., 2019). Therefore, it is likely that wells with this TOC trend were located in shallow marine, probably above or near storm wave base conditions with high oxygen content at the sea floor at MFS2, and consequently low TOC values are observed. A late Kimmerigian widespread flooding event, correlative with MFS3, has been described in the Arctic region (Koevoets et al., 2018; Smelror et al., 2001; Surlyk, 1991). Areas with TOC trend 2 became gradually deeper during the deposition of sequence 3, developing increasing upward TOC values (Figures 9 and 12a).
3. TOC trend 3: wells where MFS2 and MFS3 have similarly high TOC values are interpreted as being located in an outer shelf environment (classic depositional environment of the Hekkingen Formation; Mørk et al., 1999), during the deposition of both sequences 2 and 3 (Figures 9 and 12a; Helleren, et al., 2020). In the Hammerfest Basin, wells with this TOC trend are located in the central part. This could suggest that the

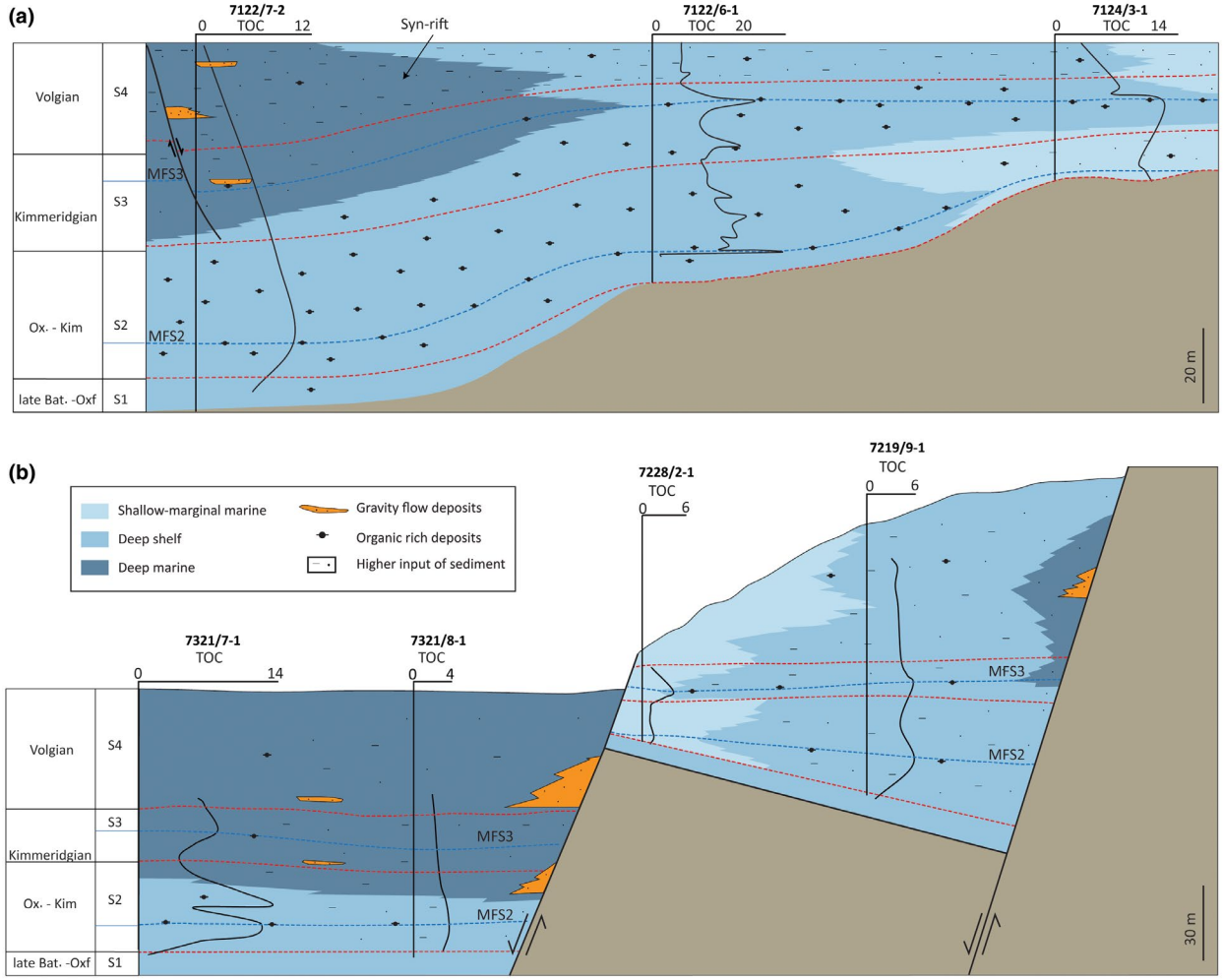

FIGURE 12 Interpretation on the controls of the three different TOC trends identified in this study. (a) Tectonically stable areas or areas affected by minor faulting. (b) Area affected by active normal faults. TOC trends are controlled by both palaeobathymetric variations and organic matter dilution

faults in this central part were not active during the deposition of sequences 2 and 3 because the sedimentation rate remained relatively constant and there is a lack of seismic wedges (Figure 11a). Wells with TOC trend 3 commonly show several minor TOC increments not only during the MFSs. Van Buchem et al. (1995) interpreted a similar pattern in wells located in the deeper part of a basin, where the variation in the TOC represents higher-order cyclicity. Seasonal events such as freshwater input and algae blooms are well documented in Svalbard (Koevoets et al., 2018; Nagy et al., 2009). These episodic events could have triggered higher productivity and anoxia in the sea bottom, explaining the variation in TOC values that are not necessarily related to relative sea-level fluctuations (Koevoets et al., 2018; Macquaker & Gawthorpe, 1993; Nagy et al., 2009).

The main regional trend in the SW Barents Sea shows that, in general, the organic-rich rocks tend to be younger in the eastern area (dominance of TOC trends 2 and 3) compared to the western area (dominance of TOC trend 1; Figure 9a). This trend is aligned with previous studies that suggest that the Upper Jurassic to lowermost Cretaceous source rocks are diachronous and becomes younger in the eastern sector of the Barents Sea (Leith et al., 1993).

6.1.2 | Areas affected by active faulting (synrift)

The three TOC trends described above were also observed in areas affected by active normal faulting or salt tectonics (i.e. wells located to the west of the Loppa High and close to the borders of the Nordkapp Basin; Figure 12b). However, fault activity is associated with lower TOC values. Fault activity controlled the TOC trends in different ways: firstly, by increasing siliciclastic input and intrinsically diluting organic matter, which led to lower TOC values (Figure 12b). Well 7220/5-2, located to the west of the Loppa High, penetrated 79 m of sequences 2 and 3, suggesting higher sedimentation rates compared to other wells located in the tectonically stable area, where the average thickness is less than 36 m (Figure 8). Larger accommodation space and higher sedimentation rates to the west of the Loppa High can also explain the high potassium content observed in well 7220/5-2 (Figure 8), as has been suggested by Paxton et al. (2007) and Abouelresh and Slatt (2012) for other regions. Secondly, fault activity controlled TOC trends, creating a fast contrast in topography. Shallow footwalls, might have reached the storm wave base, where better oxygenated sea floor decreased the potential for organic matter preservation during sequence 2 (well 7219/9-1; Figures 9c and 12b). Additionally, shallow footwalls were less likely to developed stratified waters because higher active tidal currents, compared to deep water conditions. This situation has been documented in the Kimmeridgian-Volgian Oppdalssåta Member of the Agardhfjellet Formation in Spitsbergen, where the presence of sandstone with hummocky cross-stratification coincides with well-oxygenated conditions. Anoxic conditions at the sea floor are re-established during the transgression periods (Koevoets et al., 2018). Moreover, uplifted footwalls might have contributed to trigger hyperpycnal flows increasing the input of oxygenated water to the sea floor (Lash, 2016; Macquaker & Gawthorpe, 1993).

The relative sea level rose during the deposition sequence 3, as a result of continued fault activity and the high eustatic sea level of the late Kimmeridgian (Haq, 2017), resulting in increasing upwards TOC values (well 7219/9-1; Figures 9c and 12b). It is noteworthy that TOC drops to values <6 wt % in a relatively narrow area adjacent the main fault planes. High TOC values are re-established approximately 15 km away from the main fault area in well 7321/7-1 (Figures 9c and 12b). We suggest that these three TOC trends are likely to be observed in sediment starved to sediment-balanced rift systems (Ravnås & Steel, 1998). The main difference would be related to the variation in TOC values due to dilution. The case described in this study is interpreted as a sediment-underfilled to sediment-balanced rift-system, considering the dilution of organic matter observed in the faulted blocks compared to the tectonically stable area. Thus, in other sediment-underfilled to sediment-balanced rift basins, lower TOC values are expected in the areas adjacent the main faults, where thick synrift wedge-shaped geometries are present, or in the shallow uplifted footwalls, where dilution and oxygenation are higher respectively. Higher TOC values are expected in the hanginwalls, grabens or distal areas of the basin, apart from the main master active faults. In a sediment-starved setting, we expect to observe lower organic matter dilution, and the TOC trends would be controlled by the topographic contrast caused by fault activity. The time of deposition of sequences 4 to BCU could locally represent a sediment-overfilled situation, since clinoforms and sandstone have been observed in the Hammerfest Basin, and 671 m of these sequences are penetrated in well 7219/8-1s west of the Loppa High. A higher sediment input (including sand) during the deposition of sequences 4 to BCU (late Kimmeridgian–Ryazanian, partially equivalent to the Krill Member) explains the lower TOC in these sequences observed in the Hammerfest Basin (Figure 7), even though anoxic conditions and deposition of organic-rich rocks were still prevailing in other areas of the Arctic (Georgiev et al., 2017; Leith et al., 1993). Finally, we speculate that the variation in the TOC patterns, described by Løseth et al. (2011a), may be the result of the diachronism in the Middle to Early Cretaceous rift event for the different areas of the NCS (Gabrielsen, Kyrkjebø, Faleide, Fjeldskaar, & Kjennerud, 2001).

6.2 | Palaeogeography, sediment source area size and coarse-grained input

6.2.1 | Sequence 1 (Bathonian–Oxfordian)

The absence of sequence 1 in the southern part of the study area (the south-eastern part of the Hammerfest Basin and the eastern part of the Finnmark Platform; Figure 5a) is interpreted as subaerially exposed conditions (Figure 13a). This is supported by a widespread near-base Bathonian ravinement surface in the Barents Sea and Svalbard (Berglund et al., 1986; Bugge et al., 2002; Klausen et al., 2019; Koevoets et al., 2018; Olaussen et al., 2018; Rismyhr et al., 2019). The relatively constant thickness and lack of growth strata during the Bathonian–Oxfordian imply that the Hammerfest Basin experienced minor or no fault activity. Reworked palynomorphs from Bajocian to Kimmeridgian found in the Lower Cretaceous wedges of well 7019/1-1 (see the revised biostratigraphy chapter) in the flanks of the Finnmark Platform are consistent with previously published studies from well 7120/10-2 (Marín et al., 2018b). This reworked material suggests that the western part of the Finnmark Platform was flooded during the deposition of sequence 1. Although thickness variation along the Bjørnøyrenna Fault Complex indicates fault activity, the lack of sand deposits within sequence 1 around the Loppa High may indirectly imply that this structural high was submerged.

6.2.2 | Sequences 2 and 3 (Oxfordian–Kimmeridgian)

Sequences 2 and 3 marked a regional flooding event, where local highs of Bathonian-Oxfordian were flooded. The western part of the Finnmark Platform remained flooded, which is supported by reworked palynomorphs of Kimmeridgian age in the Lower Cretaceous wedges of wells 7019/1-1 and 7120/10-2 (Marín et al., 2018b; Figure 13b). Reworked dinocyst material of the Kimmeridgian to Ryazanian age has also been observed in Lower Cretaceous wedges of wells 7120/1-2 and 7120/2-2 located in the north-western Hammerfest Basin in the flanks of the Loppa High (Marín, Escalona, Śliwińska, Nøhr-Hansen, & Mordasova, 2017). Thus, we suggest that sequences 2 and 3 were deposited on parts of the Loppa High. However, the presence of wedge-shaped geometries and thin layers of sandstone penetrated by well 7219/8-1s (NPD, 2020) indicate that fault activity continued along Bjørnøyrenna Fault Complex during the deposition of sequences 2 and 3. This fault activity led to the formation of uplifted footwall islands and localized sand deposits around these islands. We suspect that the sand coming from these islands is laterally restricted because the sediment source areas were of limited sizes. We interpret that this was the initiation of the Late Jurassic uplift of the Loppa High. This uplift event continued into the Cretaceous (Indrevær et al., 2017; Marín et al., 2018b). In the Nordkapp Basin, fault activity and salt diapirism triggered the deposition of wedges. Some of these diapirs could have been subaerially exposed.

6.2.3 | Sequences 4 to BCU (late Kimmeridgian–Ryazanian)

During this period, fault activity became important in the Hammerfest Basin, inferred by thickness variations and wedge-shaped geometries (Figures 5 and 11). The lack of Volgian reworked palynomorphs in the Lower Cretaceous wedges of wells 7019/1-1 and 7120/10-2

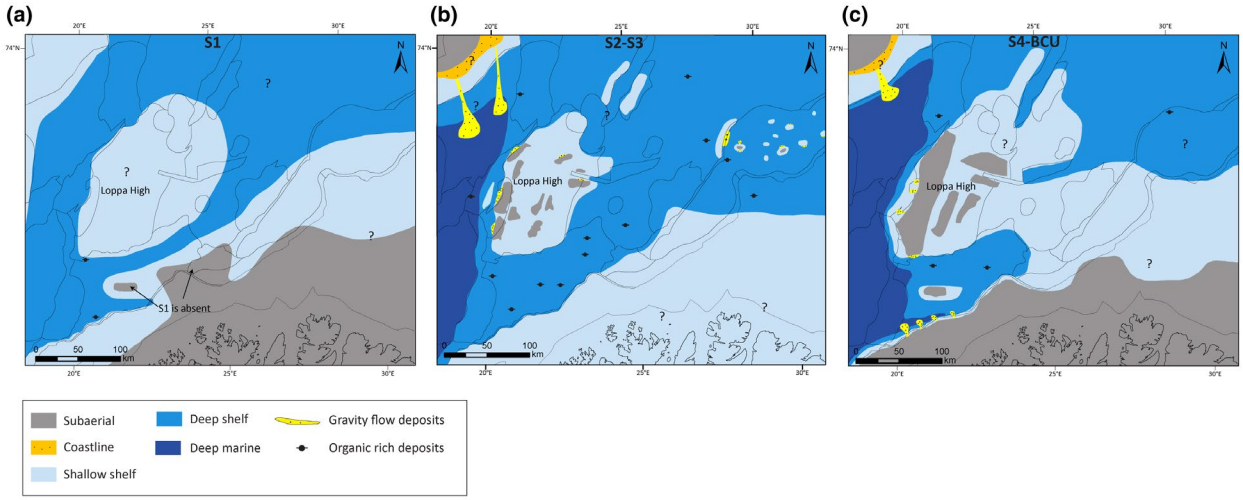

FIGURE 13 Palaeogeographic reconstructions for the south-western Barents Sea. (a) Sequence 1 (Bathonian–Oxfordian). (b) Sequences 2 and 3 (Oxfordian–late Kimmeridgian). (c) Sequences 4 to BCU (late Kimmeridgian–Ryazanian)

(Marín et al., 2018b), located in the flanks of the Finnmark Platform, suggest that Volgian sediment was not deposited on this platform. Thus, the Finnmark Platform and the central high are interpreted as uplifted related to fault activity of the Troms-Finnmark Fault Complex and other faults in the Hammerfest Basin (Figure 13c). The Loppa High is still interpreted as uplifted footwall islands, since clastic wedges indicate a source of sediment in this area, but reworked Volgian fossils in the Lower Cretaceous wedges penetrated by wells 7120/1-2 and 7120/2-2 indicate that sequence 4 was partially deposited in the high. Fault activity in the Hammerfest Basin triggered deposition of gravity flow deposits in the northern and southern parts of the basin (penetrated by wells 7120/2-2 and 7120/12-1; Braut, 2018; Sandvik, 2014). The Finnmark Platform represented a larger sediment source area and potentially delivered significant volumes of sand. Sequences 4 to BCU are condensed, missing or partially eroded in the Bjarmeland Platform. Therefore, the palaeogeography of this area is enigmatic, but probably varied from shallow marine to open marine environments.

These palaeogeographic reconstructions do not consider the role that Greenland and/or another potential source of sediment located to the northwest of the study area. However, the thickness of the Upper Jurassic succession in wells 7219/8-1s (856 m) and 7318/12-2 (516 m) in the Bjørnøya Basin could indicate an additional sediment source other than just the Loppa High islands (Figure 13b,c). This northwest source of sediments has been interpreted in Svalbard for the Kimmeridgian age (Koevoets et al., 2018), and its influence is recognized until the Barremian (Grundvåg et al., 2017).

7 | CONCLUSIONS

1. Three main TOC trends are identified based on TOC data and well logs within two main organic-rich sequences: 1) wells with decreasing upwards TOC values, where the highest TOC occurs at the base of the organic-rich succession; 2) wells with increasing upwards TOC values, where the highest TOC values are dominant at the top of the succession; 3) wells with high TOC at the base and at the top of the succession. These TOC trends are controlled by both palaeobathymetry and dilution of organic matter.
2. The three TOC trends were observed in a tectonically stable area and in an area affected by active normal faulting. The main difference between these two areas is the TOC values. Tectonically stable areas exhibit TOC values >10 wt %, whereas in areas affected by active tectonics, TOC values are <6 wt %. Fault activity controlled the TOC trends and organic matter preservation in different ways: Creating a fast contrast in topography; and increasing the clastic input, diluting the organic matter.
3. During the Late Jurassic to the earliest Cretaceous, the Loppa High was characterized by uplifted footwall islands and localized sands. The sediment source areas were of limited sizes. During the Volgian, the Finnmark Platform was properly uplifted and constituted a bigger sediment source area.

ACKNOWLEDGEMENTS

We want to thank the JuLoCrA consortium (https://wp.ux.uis.no/julocra/) for the financial support. We acknowledge the Norwegian Diskos database for providing the well and seismic database used in this study. We thank Craig Magee, Helge Løseth and two anonymous reviewers for very detailed and meticulously thought-through comments. Snorre Olaussen acknowledges the ARCEx project funded by the Research Council of Norway (grant number 228107). Authors have no conflict of interest to declare

PEER REVIEW

The peer review history for this article is available at https://publons.com/publon/10.1111/bre.12504.

DATA AVAILABILITY STATEMENT

Research data not shared.

ORCID

Dora Marín https://orcid.org/0000-0001-8006-9638
Solveig Helleren https://orcid.org/0000-0002-8434-6011
Snorre Olaussen https://orcid.org/0000-0002-7922-8010

REFERENCES

Abouelresh, M. O., & Slatt, R. M. (2012). Lithofacies and sequence stratigraphy of the Barnett shale in east-central fort worth basin, texasgeohorizon. *AAPG Bulletin*, *96*, 1–22.

Århus, N. (1991). The transition from deposition of condensed carbonates to dark claystones in the Lower Cretaceous succession of the Southwestern Barents Sea. *Norsk Geologisk Tidsskrift*, *71*, 259.

Berglund, L., Augustson, J., Færseth, R., Gjelberg, J., & Ramberg-Moe, H. (1986) The Evolution of the Hammerfest Basin. In: A. M. Spencer (Ed.) Habitat of Hydrocarbons on the Norwegian Continental Shelf. *Norwegian Pet. Soc. Graham Trotman*, 319–338.

Blaich, O. A., Tsikalas, F., & Faleide, J. I. (2017). New insights into the tectono-stratigraphic evolution of the southern Stappen high and its transition to Bjørnøya Basin, Sw Barents Sea. *Marine and Petroleum Geology*, *85*, 89–105. https://doi.org/10.1016/j.marpetgeo.2017.04.015

Bohacs, K. M., Grabowski, G. J., Carroll, A. R., Mankiewicz, P. J., Miskell-Gerhardt, K. J., Schwalbach, J. R., …Simo, J. A. (2005). Production, destruction, and dilution—the many paths to source-rock development. The Deposition of Organic-Carbon-Rich Sediments: Models, Mechanisms, and Consequences. N. B. Harris. *SEPM Society for Sedimentary Geology*, *82*, 61–101.

Bowker, K. A., & Grace, T. (2010). The downside of using GR to determine TOC content: An example from the Marcellus Shale in SE West Virginia. Critical assessment of shale resource plays: Presented at AAPG Hedberg Research Conference

Braut, T. I.(2018). Middle to Upper Jurassic Depositional Setting in the Hammerfest Basin, Southwestern Barents Sea. Master thesis, University of Stavanger, 106.

Bugge, T., Elvebakk, G., Fanavoll, S., Mangerud, G., Smelror, M., Weiss, H. M., … Nilsen, K. (2002). Shallow stratigraphic drilling applied in hydrocarbon exploration of the Nordkapp Basin, Barents Sea. *Marine and Petroleum Geology*, *19*, 13–37. https://doi.org/10.1016/S0264-8172(01)00051-4

Catuneanu, O., Abreu, V., Bhattacharya, J., Blum, M., Dalrymple, R., Eriksson, P., … Gibling, M. (2009). Towards the standardization of sequence stratigraphy. *Earth-Science Reviews*, *92*, 1–33. https://doi.org/10.1016/j.earscirev.2008.10.003

Chiarella, D., Longhitano, S. G., Mosdell, W., & Telesca, D. (2020). Sedimentology and facies analysis of ancient sand ridges: Jurassic Rogn Formation, trøndelag platform, Offshore Norway. *Marine and Petroleum Geology*, *112*, 104082. https://doi.org/10.1016/j.marpetgeo.2019.104082

Clark, S.,Glorstad-Clark, E.,Faleide, J., Schmid, D., Hartz, E., & Fjeldskaar, W. (2014). Southwest Barents Sea rift basin evolution: comparing results from backstripping and time-forward modelling. *Basin Research*, *26*, 550–566. https://doi.org/10.1111/bre.12039

Costa, L. I., & Davey, R. J. (1992). Dinoflagellate cysts of the Cretaceous system. In A. J. Powell (Ed.), *A stratigraphic index of dinoflagellate cysts* (pp. 99–131). London: Chapman and Hall, 99–131.

Creaney, S., & Passey, Q. R. (1993). Recurring patterns of total organic carbon and source rock quality within a sequence stratigraphic framework. *AAPG Bulletin*, *77*, 386–401.

Dalland, A., Worsley, D., & Ofstad, K. (1988). A lithostratigraphic scheme for the Mesozoic and Cenozoic succession offshore Norway North of 62 N. *NPD Bulletin.*, *4*, 67.

Davies, S. J., & Elliott, T. (1996). Spectral gamma ray characterization of high resolution sequence stratigraphy: examples from upper Carboniferous fluvio-deltaic systems, County Clare, Ireland. *Geological Society, London, Special Publications*, *104*, 25–35. https://doi.org/10.1144/GSL.SP.1996.104.01.03

Demaison, G. J., & Moore, G. T. (1980). Anoxic environments and oil source bed genesis. *AAPG Bulletin*, *64*, 1179–1209.

Embry, A. (2009). Practical sequence stratigraphy. *Canadian Society of Petroleum Geologists*, *81*, 79. www.cspg.org

Emery, D., & Myers, K. (2009). *Sequence stratigraphy* (p. 264). Oxford: John Wiley & Sons.

Faleide, J. I., Vågnes, E., & Gudlaugsson, S. T. (1993). Late Mesozoic-Cenozoic evolution of the South-Western Barents Sea in a regional rift-shear tectonic setting. *Marine and Petroleum Geology*, *10*, 186–214. https://doi.org/10.1016/0264-8172(93)90104-Z

Faleide, T. S., Midtkandal, I., Planke, S., Corseri, R., Faleide, J. I., Serck, C. S., & Nystuen, J. P. (2019). Characterisation and development of early cretaceous shelf platform deposition and faulting in the hoop area, southwestern barents sea-constrained by high-resolution seismic data. *Norwegian Journal of Geology*, *99*, 1–20. https://doi.org/10.17850/njg99-3-7

Gabrielsen, R. H., Kyrkjebø, R., Faleide, J. I., Fjeldskaar, W., & Kjennerud, T. (2001). The Cretaceous post-rift basin configuration of the Northern North Sea. *Petroleum Geoscience*, *7*, 137–154. https://doi.org/10.1144/petgeo.7.2.137

Georgiev, S. V., Stein, H. J., Hannah, J. L., Xu, G., Bingen, B., & Weiss, H. M. (2017). Timing, duration, and causes for Late Jurassic-Early Cretaceous anoxia in the Barents Sea. *Earth and Planetary Science Letters*, *461*, 151–162. https://doi.org/10.1016/j.epsl.2016.12.035

Gernigon, L., Brönner, M., Roberts, D., Olesen, O., Nasuti, A., & Yamasaki, T. (2014). Crustal and basin evolution of the southwestern Barents Sea: from caledonian orogeny to continental breakup. *Tectonics*, *33*, 347–373. https://doi.org/10.1002/2013TC003439

Glørstad-Clark, E.(2010). Basin analysis in the western Barents Sea area: the interplay between accommodation space and depositional systems. PhD Thesis. University of Oslo, 212.

Goesten, M., & Nelson, P. (1992) Draugen Field-Norway North Sea Basin, Haltenbanken Area. In: Structural Traps VI (Ed. By Foster N.H. & Beaumont E.A.). *AAPG*, 37–54.

Grundvåg, S. A., Marin, D., Kairanov, B., Śliwińska, K. K., Nøhr-Hansen, H., Jelby, M. E., … Olaussen, S. (2017). The Lower Cretaceous succession of the northwestern barents shelf: onshore and offshore correlations. *Marine and Petroleum Geology*, *86*, 834–857. https://doi.org/10.1016/j.marpetgeo.2017.06.036

Haq, B. U. (2017). Jurassic sea-level variations: a reappraisal. *GSA Today*, *28*, 4–10.

Helleren, S., Marín, D., Ohm, S., Augustsson, C., & Escalona, A. (2020). Why does not lithology correlate with gamma-ray spikes in the shaley source rocks of the Upper Jurassic Alge Member (southwestern Barents Sea)? *Marine and Petroleum Geology*, *121*, 104623–https://doi.org/10.1016/j.marpetgeo.2020.104623

Hemmesch, N. T., Harris, N. B., Mnich, C. A., & Selby, D. (2014). A sequence-stratigraphic framework for the upper Devonian woodford shale, permian basin, west texassequence stratigraphy, woodford shale, permian basin, Texas. *AAPG Bulletin*, *98*, 23–47.

Henriksen, E., Ryseth, A., Larssen, G., Heide, T., Rønning, K., Sollid, K., & Stoupakova, A. (2011). Tectonostratigraphy of the greater Barents Sea: implications for petroleum systems. *Geological Society, London, Memoirs*, *35*, 163–195.

Herbin, J. P., Fernandez-Martinez, J. L., Geyssant, J. R., Albani, A. E., Deconinck, J. F., Proust, J. N., … Vidier, J. P. (1995). Sequence stratigraphy of source rocks applied to the study of the Kimmeridgian/Tithonian in the North-West European Shelf (Dorset/Uk, Yorkshire/Uk and Boulonnais/France). *Marine and Petroleum Geology*, *12*, 177–194. https://doi.org/10.1016/0264-8172(95)92838-N

Huc, A., le Fournier, J., Vandenbroucke, M., & Bessereau, G. (1990) Northern Lake Tanganyika–an Example of Organic Sedimentation in an Anoxic Rift Lake: Chapter 10. In: Lacustrine Basin Exploration: Case Studies and Modern Analogs (Ed. by Katz B.J) *AAPG Memoirs*, *50*, 169–185.

Hunt, J. M. (1995). *Petroleum geochemistry and geology* (p. 743). New York: Freeman.

Indrevær, K., Gabrielsen, R. H., & Faleide, J. I. (2017). Early Cretaceous synrift uplift and tectonic inversion in the Loppa high area, southwestern Barents sea, Norwegian shelf. *Journal of the Geological Society*, *174*, 242–254. https://doi.org/10.1144/jgs2016-066

Josefsen, O.(2019). Origin of anticline structure in the southern Hammerfest Basin and their impact in sedimentation and coarse-grained distribution. Master thesis. University of Stavanger, 81 p.

Kairanov, B., Marín, D., Escalona, A., & Cardozo, N. (2019). Growth and linkage of a basin-bounding fault system: insights from the Early Cretaceous evolution of the Northern Polhem Subplatform, SW Barents Sea. *Journal of Structural Geology*, *124*, 182–196. https://doi.org/10.1016/j.jsg.2019.04.014

Katz, B. J. (1995). A survey of rift basin source rocks. *Geological Society, London, Special Publications*, *80*, 213–240. https://doi.org/10.1144/GSL.SP.1995.080.01.11

Khan, S. A., Ansari, K. G. M. T., & Lyla, P. S. (2012). Organic matter content of sediments in continental shelf area of southeast coast of India. *Environmental Monitoring and Assessment*, *184*, 7247–7256. https://doi.org/10.1007/s10661-011-2494-8

Klausen, T. G., Müller, R., Poyatos-Moré, M., Olaussen, S., & Stueland, E. (2019). Tectonic, provenance and sedimentological controls on reservoir characteristics in the Upper Triassic-Middle Jurassic Realgrunnen Subgroup, Sw Barents Sea. *Geological Society, London, Special Publications*, *495*, 2018-2165. https://doi.org/10.1144/SP495-2018-165

Koevoets, M. J., Hammer, Ø., Olaussen, S., Senger, K., & Smelror, M. (2018). Integrating subsurface and outcrop data of the Middle Jurassic to Lower cretaceous Agardhfjellet formation in central Spitsbergen. *Norwegian Journal of Geology*, *98*, 1–34. https://doi.org/10.17850/njg98-4-01

Lash, G. G. (2016). Hyperpycnal transport of carbonaceous sediment-example from the upper Devonian Rhinestreet shale, Western New York, USA. *Palaeogeography, Palaeoclimatology, Palaeoecology*, *459*, 29–43. https://doi.org/10.1016/j.palaeo.2016.06.035

Leith, T., Weiss, H., Mørk, A., Elvebakk, G., Embry, A., Brooks, P., … Verba, M. (1993). Mesozoic hydrocarbon source-rocks of the Arctic region. In T. O. Vorren, E. Bergsager, Ø. A. Dahl-Stamnes, E. Holter, B. Johansen, E. Lie & T. B. Lund (Eds.), *Norwegian petroleum society special publications* (Vol. *2*, pp. 1–25). Elsevier.

Lerch, B., Karlsen, D., Matapour, Z., Seland, R., & Backer-Owe, K. (2016). Organic geochemistry of barents sea petroleum: thermal maturity and alteration and mixing processes in oils and condensates. *Journal of Petroleum Geology*, *39*, 125–148. https://doi.org/10.1111/jpg.12637

Lerch, B., Karlsen, D. A., Thieβen, O., Abay, T. B., van Soelen, E. E., Kürschner, W. M., … Backer-Owe, K. (2018). Investigations on the use of triaromatic dimethylcholesteroids as age-specific biomarkers in bitumens and oils from arctic Norway. *Organic Geochemistry*, *122*, 1–16. https://doi.org/10.1016/j.orggeochem.2018.04.011

Løseth, H., Wensaas, L., & Gading, M. (2011b). Deformation structures in organic-rich shales. *AAPG Bulletin*, *95*, 729–747. https://doi.org/10.1306/09271010052

Løseth, H., Wensaas, L., Gading, M., Duffaut, K., & Springer, M. (2011a). Can hydrocarbon source rocks be identified on seismic data? *Geology*, *39*, 1167–1170. https://doi.org/10.1130/G32328.1

Macquaker, J., & Gawthorpe, R. (1993). Mudstone lithofacies in the kimmeridge clay formation, Wessex Basin, Southern England; implications for the origin and controls of the distribution of mudstones. *Journal of Sedimentary Research*, *63*, 1129–1143.

Marín, D., Escalona, A., Grundvåg, S.-A., Nøhr-Hansen, H., & Kairanov, B. (2018a). Effects of adjacent fault systems on drainage patterns and evolution of uplifted rift shoulders: the Lower Cretaceous in the Loppa high, Southwestern Barents Sea. *Marine and Petroleum Geology*, *94*, 212–229. https://doi.org/10.1016/j.marpetgeo.2018.04.009

Marín, D., Escalona, A., Grundvåg, S.-A., Olaussen, S., Sandvik, S., & Śliwińska, K. K. (2018b). Unravelling key controls on the rift climax to post-rift fill of marine rift basins: insights from 3d seismic analysis of the Lower Cretaceous of the Hammerfest Basin, Sw Barents Sea. *Basin Research*, *30*, 587–612. https://doi.org/10.1111/bre.12266

Marín, D., Escalona, A., Śliwińska, K. K., Nøhr-Hansen, H., & Mordasova, A. (2017). Sequence stratigraphy and lateral variability of Lower Cretaceous Clinoforms in the Southwestern Barents Sea. *AAPG Bull.*, *101*, 1487–1517.

Martins-Neto, M. A., & Catuneanu, O. (2010). Rift sequence stratigraphy. *Marine and Petroleum Geology*, *27*, 247–253. https://doi.org/10.1016/j.marpetgeo.2009.08.001

Miller, K. G., Mountain, G. S., Browning, J. V., Katz, M. E.,Monteverde, D., Sugarman, P. J., … Hodgson, D. (2013). Testing sequence stratigraphic models by drilling Miocene foresets on the New Jersey shallow shelf. *Geosphere*, *9*, 1236–1256. https://doi.org/10.1130/GES00884.1

Mitchum, R. Jr, Vail, P., & Sangree, J. (1977) Seismic stratigraphy and global changes of sea level: Part 6. stratigraphic interpretation of seismic reflection patterns in depositional sequences: Section 2. In: Application of Seismic Reflection Configuration to Stratigraphic Interpretation (Ed. by Payton C.E.) *AAPG Memoirs*, *26*, 117–133.

Mørk, A., Dallmann, W., Dypvik, H., Johannessen, E., Larssen, G., Nagy, J., … Worsley, D. (1999). Mesozoic Lithostratigraphy. Lithostratigraphic lexicon of Svalbard. Upper Palaeozoic to Quaternary bedrock. In W. K. Dallmann (Ed.), *Review and recommendations for nomenclature use* (pp. 127–214). Tromsø: Norwegian Polar Institute.

Mulrooney, M. J., Leutscher, J., & Braathen, A. (2017). A 3d structural analysis of the Goliat field, Barents Sea, Norway. *Marine and Petroleum Geology*, *86*, 192–212. https://doi.org/10.1016/j.marpetgeo.2017.05.038

Mulrooney, M. J., Rismyhr, B., Yenwongfai, H. D., Leutscher, J., Olaussen, S., & Braathen, A. (2018). Impacts of small-scale faults on continental to coastal plain deposition: evidence from the Realgrunnen Subgroup in the Goliat field, Southwest Barents Sea, Norway. *Marine and Petroleum Geology*, *95*, 276–302. https://doi.org/10.1016/j.marpetgeo.2018.04.023

Myers, K. J., & Wignall, P. B. (1987). Understanding Jurassic Organic-Rich Mudrocks—New Concepts Using Gamma-Ray Spectrometry and Palaeoecology: Examples from the Kimmeridge Clay of Dorset and the Jet Rock of Yorkshire. In: Marine Clastic Sedimentology (Ed. by Legget J.K., & Zuffa G.G.), 172–189. Springer.

Nagy, J., Reolid, M., & Rodríguez-Tovar, F. J. (2009). Foraminiferal morphogroups in dysoxic shelf deposits from the Jurassic of Spitsbergen. *Polar Research*, *28*, 214–221. https://doi.org/10.1111/j.1751-8369.2009.00112.x

Nøhr-Hansen, H. (1993). Dinoflagellate cyst stratigraphy of the barremian to Albian, Lower Cretaceous, North-East Greenland. *Grønlands Geologiske Undersøgelse Bulletin*, *166*, 171.

NPD (2020) Norwegian Petroleum Directorate Factpages. Retrieved from http://factpages.npd.no/factpages/Default.aspx?culture=en

Ohm, S. E., Karlsen, D. A., & Austin, T. (2008). Geochemically driven exploration models in uplifted areas: Examples from the norwegian Barents Sea. *AAPG Bulletin*, *92*, 1191–1223. https://doi.org/10.1306/06180808028

Olaussen, S., Larssen, G. B., Helland-Hansen, W., Johannessen, E. P., Nøttvedt, A., Riis, F., … Worsley, D. (2018). Mesozoic strata of Kong Karls Land, Svalbard, Norway; a link to the northern Barents Sea basins and platforms. *Norwegian Journal of Geology*, *98*, 1–69.

Passey, Q., Creaney, S., Kulla, J., Moretti, F., & Stroud, J. (1990). A practical model for organic richness from porosity and resistivity logs. *AAPG Bulletin*, *74*, 1777–1794.

Paxton, S. T., Aufill, M., Cruse, A. M., Puckette, J. O., Hurst, D. D., & Samson, T. (2007). *Use of spectral gamma ray profiles for*

discriminating depositional and stratigraphic successions in upper devonian-lower mississippian gas shale intervals. GSA Denver Annual Meeting: North America.

Prosser, S. (1993). Rift-related linked depositional systems and their seismic expression. *Geological Society, London, Special Publications*, *71*(1), 35–66. https://doi.org/10.1144/GSL.SP.1993.071.01.03

Ravnås, R., & Steel, R. J. (1997). Contrasting styles of Late Jurassic syn-rift turbidite sedimentation: a comparative study of the Magnus and Oseberg areas, Northern North Sea. *Marine and Petroleum Geology*, *14*, 417–449. https://doi.org/10.1016/S0264-8172(97)00010-X

Ravnås, R., & Steel, R. J. (1998). Architecture of marine rift basin successions. *AAPG Bulletin*, *82*, 110–146.

Rider, M. H. (1996). *The geological interpretation of wireline logs*, 2nd ed. Scotland: Whittles Publishing, 280 p.

Riding, J. B. (1994). A taxonomic study of the Mesozoic dinoflagellate cysts Phallocysta elongata (Beju 1971) comb. nov., emend. nov. and Wallodinium cylindricum (Habib 1970) Duxbury 1983 emend. *Nov. Palynology*, *18*, 11–22.

Riding, J. B.,& Fensome, R. A. (2002). A review of Scriniodinium Klement 1957, Endoscrinium (Klement 1960) Vozzhennikova 1967 and related dinoflagellate cyst taxa. *Palynology*, *26*, 5–33.

Rismyhr, B., Bjærke, T., Olaussen, S., Mulrooney, M. J., & Senger, K. (2019). Facies, Palynostratigraphy and Sequence Stratigraphy of the Wilhelmøya Subgroup (Upper Triassic-Middle Jurassic) in Western Central Spitsbergen, Svalbard. *Norwegian Journal of Geology*, *99*, 35–64.

Rojo, L. A., Cardozo, N., Escalona, A., & Koyi, H. (2019). Structural style and evolution of the Nordkapp Basin, Norwegian Barents Sea. *AAPG Bulletin*, *103*, 2177–2217.

Sandvik, S.(2014). Description and comparison of lower cretaceous deposits from Svalbard and the southern Loppa high. Master thesis, University of Bergen, 135.

Scott, A. S., & Ottesen, S. (2018) Tectono-Stratigraphic Development of the Upper Jurassic in the Johan Sverdrup Field Area, Norwegian North Sea. In: Rift-related coarse-grained submarine fan reservoirs; the Brae Play, South Viking Graben, North Sea (Ed. By Turner C.C & Cronin B.T.), *AAPG Memoirs*, *115*, 445–452.

Serck, C. S., Faleide, J. I., Braathen, A., Kjølhamar, B., & Escalona, A. (2017). Jurassic to Early Cretaceous Basin Configuration(S) in the Fingerdjupet Subbasin, SW Barents Sea. *Marine and Petroleum Geology*, *86*, 874–891. https://doi.org/10.1016/j.marpetgeo.2017.06.044

Smelror, M., Below, R. et al (1993). Dinoflagellate biostratigraphy of the Toarcian to Lower Oxfordian (Jurassic) of the Barents Sea region. In T. O. Vorren (Ed.), *Arctic geology and petroleum potential. NPF special publication 2* (pp. 495–513). Elsevier Scientific Publications.

Smelror, M., & Dypvik, H. (2005). Marine microplankton biostratigraphy of the Volgian-Ryazanian Boundary strata, western barents shelf. *NGU Bulletin*, *443*, 61–69.

Smelror, M., Mørk, A., Mørk, M. B. E., Weiss, H. M., & Løseth, H. (2001). Middle Jurassic-Lower Cretaceous transgressive-regressive sequences and facies distribution off Northern Nordland and Troms, Norway. *Norwegian Petroleum Society Special Publications*, *10*, 211–232.

Sund, T., Skarpnes, O., Jensen, L. N., & Larsen, R. M. (1986). Tectonic development and hydrocarbon potential offshore Troms, Northern Norway. In: Future Petroleum Provinces of the World (Ed. by Halbouty M.T.), *AAPG Memoirs*, *40*, 615–627.

Surlyk, F. (1991). Sequence stratigraphy of the Jurassic-lowermost Cretaceous of East Greenland. *AAPG Bulletin*, *75*, 1468–1488.

Tissot, B., & Welte, D. (1984). *Petroleum Formation and Occurrence*. Berlin Heidelberg: Springer. 702 p.

Turner, C. C., & Hooper, R. J. (2018). Gravity-Driven Versus Inversion Origins for Upper Jurassic Trapping Structures of the Brae Fields, South Viking Graben, Uk North Sea. In: Rift-related coarse-grained submarine fan reservoirs; the Brae Play, South Viking Graben, North Sea (Ed. by Turner C.C & Cronin B.T.), *AAPG Memoirs*, *115*, 565–594.

Tyson, R. V. (1996). Sequence-stratigraphical interpretation of organic facies variations in marine siliciclastic systems: general principles and application to the Onshore Kimmeridge Clay Formation, UK. *Geological Society of London Special Publications*, *103*, 75–96. https://doi.org/10.1144/GSL.SP.1996.103.01.06

Tyson, R. V.,& Pearson, T. H. (1991). Modern and ancient continental shelf anoxia: an overview. *Geological Society of London Special Publications*, *58*, 1–24. https://doi.org/10.1144/GSL.SP.1991.058.01.01

Usken, B.(2018). Upper Jurassic-Lower Cretaceous seismic interpretation in the Nysleppen Fault complex, SW Barents Sea. Bachelor thesis. University of Stavanger, 58 p.

van Buchem, E. S. P., Herbin, J.-P., de Boer, P. L., McCave, I. N., & Huc, A.-Y. (1995). The Organic Carbon Distribution in Mesozoic Marine Sediments and the Influence of Orbital Climatic Cycles (England and the Western North Atlantic). In: Paleogeography, Paleoclimate, and Source Rocks (Ed. by Huc A.Y.), 40, 0. American Association of Petroleum Geologists.

Wierzbowski, A., & Århus, N. (1990). Ammonite and dinoflagellate cyst succession of an upper Oxfordian-Kimmeridgian black shale core from the Nordkapp Basin, Southern Barents Sea. *Newsletters on Stratigraphy*, *22*, 7–19. https://doi.org/10.1127/nos/22/1990/7

Wierzbowski, A., & Smelror, M. (2020). The Bajocian to Kimmeridgian (Middle to Upper Jurassic) Ammonite Succession at Sentralbanken High (Core 7533/3-U-1), Barents Sea, and Its Stratigraphical and Palaeobiogeographical Significance. *Volumina Jurassica*, *18*, 1–22. https://doi.org/10.7306/vj.18.1

SUPPORTING INFORMATION

Additional supporting information may be found online in the Supporting Information section.

How to cite this article: Marín D, Helleren S, Escalona A, et al. The Middle Jurassic to lowermost Cretaceous in the SW Barents Sea: Interplay between tectonics, coarse-grained sediment supply and organic matter preservation. *Basin Res*. 2020;00:1–23. https://doi.org/10.1111/bre.12504